

Color it, Code it, Cancel it: k -local dynamical decoupling from classical additive codes

Minh T. P. Nguyen,^{1,*} Maximilian Rimbach-Russ,¹ and Stefano Bosco^{1,†}

¹QuTech and Kavli Institute of Nanoscience, Delft University of Technology, Lorentzweg 1, 2628 CJ Delft, The Netherlands

Dynamical decoupling is a central technique in quantum computing for actively suppressing decoherence and systematic imperfections through sequences of single-qubit operations. Conventional sequences typically aim to completely freeze system dynamics, often resulting in long protocols whose length scales exponentially with system size. In this work, we introduce a general framework for constructing time-optimal, selectively-tailored sequences that remove only specific local interactions. By combining techniques from graph coloring and classical coding theory, our approach enables compact and hardware-tailored sequences across diverse qubit platforms, efficiently canceling undesired Hamiltonian terms while preserving target interactions. This opens up broad applications in quantum computing and simulation. At the core of our method is a mapping between dynamical decoupling sequence design and error-detecting codes, which allows us to leverage powerful coding-theoretic tools to construct customized sequences. To overcome exponential overheads, we exploit symmetries in colored interaction hypergraphs, extending graph-coloring strategies to arbitrary many-body Hamiltonians. We demonstrate the effectiveness of our framework through concrete examples, including compact sequences that suppress residual ZZ and ZZZ interactions in superconducting qubits and Heisenberg exchange coupling in spin qubits. We also show how it enables Hamiltonian engineering by simulating the anisotropic Kitaev honeycomb model using only isotropic Heisenberg interactions.

I. INTRODUCTION

Dynamical decoupling (DD), originally inspired by nuclear magnetic resonance [1–5], has become a powerful technique in quantum information processing. Traditionally, DD has been employed to mitigate imperfections in near-term quantum devices by using sequences of single-qubit operations to isolate quantum systems from environmental noise [6–9]. Sequences that suppress on-site decoherence to high order in time include for example universal single-qubit protocols [7, 8], XY family [10–12], concatenated sequences [13, 14], and the Uhrig family [15–17]. DD has also found applications in quantum sensing, such as frequency-selective spectroscopy [18, 19], and in quantum error correction [20, 21].

Beyond decoherence, DD protocols have been effective in suppressing systematic errors originating from high-order qubit interactions, such as residual crosstalk [22–24] from two-body couplings, leading to advanced sequences such as WAHUA [25] and fractal decoupling [26]. However, these methods were designed primarily for small systems with limited connectivity. Recent advances aim to develop time-efficient DD sequences that scale to large systems with arbitrary connectivity graphs [24, 27, 28]. Moreover, while conventional DD sequences typically freeze the system dynamics entirely, making them difficult to adapt for designing specific quantum evolutions, recent developments have proposed DD protocols for quantum simulation, including the engineering of target Hamiltonians using average Hamiltonian theory [29].

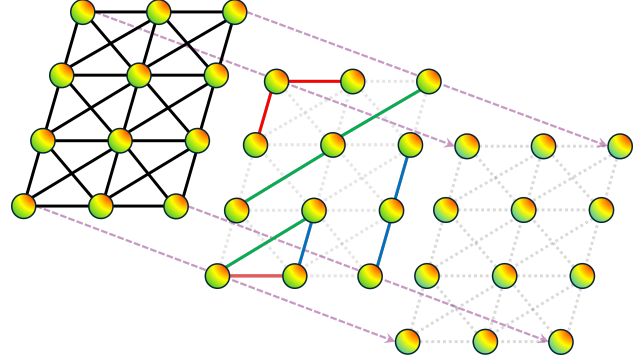


FIG. 1: **Canceling local interactions by dynamical decoupling.** Our framework permits an efficient and selective suppression of local interactions. For example, by applying tailored DD sequences to a device with dense connectivity (top), we can separate the system into non-interacting clusters, preserving only certain interactions within each cluster (middle), or completely freezing the system’s dynamics (bottom). Our framework also applies to general interactions graphs going beyond nearest neighbor and is not restricted to instantaneous control pulses.

In this work, we present a unified framework that leverages graph coloring and coding theory to construct time-efficient DD sequences capable of selectively canceling specific local interactions. Crucially, our approach reveals a connection between DD and classical error-detecting codes, allowing classical additive codes to be translated into scalable DD protocols tailored for general k -local Hamiltonians [30]. Our framework also supports finite-width pulses with bounded-strength control [31], lifting the need for idealized instantaneous (bang-bang) operations [7].

* m.t.phamnguyen@tudelft.nl
 † s.bosco@tudelft.nl

We begin by identifying a hidden symmetry in the underlying hypergraph coloring problem, which reduces complexity by grouping qubits into equivalence color classes. The efficient DD sequences for these classes are then systematically constructed using classical additive codes. Our framework generalizes and unifies existing approaches [24, 27, 28, 30, 32] while opening promising avenues for quantum simulation and control, as sketched in Fig. 1. These include universal DD protocols that suppress both decoherence and k -local residual interactions, as well as the dynamical design of effective Hamiltonians with tailored interactions. This capability has deep implications for near-term quantum computing and simulations, permitting e.g. detailed studies of dynamical phases of matters such as time crystals. Furthermore, mapping DD sequences to classical detection codes can aid in discovering robust sequences using machine learning [33, 34], by significantly reducing the search space for sequences tailored to specific tasks, and potentially providing an efficient means to generate large datasets of decoupling sequences for training.

This manuscript is organized as follows. In Sec. II, we briefly review bang-bang dynamical decoupling, emphasizing the connection between DD sequences and group theory. In Sec. III, we reinterpret the results of Refs. [24, 27] by uncovering a hidden symmetry structure in colored interaction graphs and extend this perspective to general k -local Hamiltonians. In Sec. IV, we establish the correspondence between DD sequences and classical additive codes. Sec. V presents two applications that explicitly demonstrate the power of our framework: (i) a general time-efficient decoupling protocol for two- and three-local interactions tailored to superconducting and spin qubits, and (ii) a DD sequence permitting quantum simulating of the Kitaev honeycomb model, which strongly relies on anisotropic interactions, using only isotropic Heisenberg exchange interactions.

II. DECOUPLING SEQUENCE FROM GROUP THEORY

A. Dynamical decoupling

DD offers a general framework for suppressing unwanted interactions arising from arbitrary Hamiltonians by applying sequences of quantum gates. This approach is traditionally employed in scenarios where a quantum system is weakly coupled to an environment, with the objective that, after the DD sequence, the influence of the environment on the system is effectively canceled. In particular, we consider the Hamiltonian [7]

$$H_{tot} = H_S + H_E + H_{SE}, \quad (1)$$

that couples a qubit system with Hamiltonian H_S to an environment H_E by the interaction H_{SE} . Without loss

of generality, we assume that

$$H_{SE} = \sum_i P_i \otimes O_i, \quad (2)$$

where P_i is a string of Pauli operators acting on the system and O_i is an operator acting on the environment.

The DD problem involves designing a control Hamiltonian $H_c(t)$ acting solely on the system that suppresses the interactions with the environment. This means that after the applying $H_c(t)$, the joint system-environment dynamics are governed by the decoupled Hamiltonian

$$\bar{H}_{tot} = \bar{H}_S + \bar{H}_E, \quad (3)$$

where \bar{H}_S (\bar{H}_E) denotes a (possibly) modified system (environment) Hamiltonian.

We restrict ourselves to the analysis of control Hamiltonians comprising sequences that alternate between fast single-qubit gates and free evolution intervals, where all free-evolution intervals have the same duration. These admit a natural group-theoretic description and are especially advantageous for compilation, as they simplify both the implementation and analysis of control protocols. In these cases, the effective Hamiltonian \bar{H}_{tot} can be systematically derived using tools such as Floquet theory and Magnus expansion, assuming that the expansion converges [35].

To do so, we denote the time-evolution operator generated by the control Hamiltonian $U_c(t)$ associated with $H_c(t)$ as

$$U_c(t) = \mathcal{T} \exp \left[-i \int_0^t H_c(t') dt' \right], \quad (4)$$

where \mathcal{T} is the time ordering operator and we set $\hbar = 1$. If the control Hamiltonian is cyclic with period T_c , i.e., $H_c(t) = H_c(t + T_c)$, and the initial time is at $t = 0$, the stroboscopic time evolution of the system and bath at times nT_c with $n \in \mathbb{N}$ is described by [36, 37]

$$U(nT_c) = \exp \left(-inT_c \bar{H}_{tot} \right) \quad (5)$$

where \bar{H}_{tot} is a time-independent stroboscopic Hamiltonian.

When the frequency $1/T_c$ is larger than the largest energy scale of the interaction to be removed [38], the effective Hamiltonian \bar{H}_{tot} is well approximated by the first-order Magnus expansion

$$\bar{H}_{tot} \approx \frac{1}{T_c} \int_0^{T_c} U_c^\dagger(t) H_{tot} U_c(t) dt. \quad (6)$$

Higher-order corrections in the Magnus expansion can be systematically bounded using Lemma 4 of Ref. [38].

In this work, we aim to generalize this concept. Rather than focusing solely on suppressing interactions with the environment, our objective is to design DD sequences that can also selectively suppress certain interactions

within the system itself. For example, we either completely freeze the system dynamics (i.e., $\bar{H}_S = 0$) or we selectively retain only some desired interactions in H_S , thereby engineering specific target Hamiltonians. This capability is particularly useful for digital-analog quantum simulations [39].

In the next section, we will briefly review the bang-bang control scheme [7, 8], which enables a simple design of DD sequences using group theory. In Appendix A, we also review the bounded-strength control scheme [31], that provides a more realistic model assuming that single-qubit gates have a finite duration. Importantly, we emphasize that the framework we introduce in this work applies to both control schemes.

B. Bang-bang control sequence

The bang-bang control scheme [7, 8] assumes that single-qubit pulses are instantaneous. The central idea is to define a DD group $\mathcal{G} = \{g_i\}$ [7, 24, 31], which acts on the system Hilbert space via a unitary representation $g \rightarrow U_g$. The bang-bang DD sequence is then specified by an ordered list of group elements (g_1, g_2, \dots, g_L) , with total length of the sequence $L = \lambda|\mathcal{G}|$, where $|\mathcal{G}|$ is the order of the group and λ is a positive integer, typically $\lambda = 1$ [31]. In general, each group element $g_i \in \mathcal{G}$ appears exactly λ times in the sequence.

A single cycle of the bang-bang control unitary $U_c(t)$ has a total duration T_c and is defined as a step function of time divided into L equally-spaced intervals of length $\Delta = T_c/L$. During each segment, lasting for a time $\tau \in [0, \Delta)$, the control is a constant unitary operator

$$U_c[(j-1)\Delta + \tau, (j-1)\Delta] = U_{g_j}. \quad (7)$$

This control unitary is abruptly switched from $U_{g_{j-1}}$ to U_{g_j} , corresponding to an ideal instantaneous control pulse [7, 31].

Under the action of the DD group \mathcal{G} , the effective Hamiltonian \bar{H}_{tot} in Eq. (6), is given by the group twirling operation

$$\bar{H}_{tot} = \frac{1}{|\mathcal{G}|} \sum_{g \in \mathcal{G}} U_g^\dagger H_{tot} U_g := \Pi_{\mathcal{G}}(H_{tot}). \quad (8)$$

The time-evolution operator of \bar{H}_{tot} , corresponding to the time-evolution of H_{tot} at the stroboscopic times nT_c , is explicitly given by

$$U(nT_c) \approx \left(\prod_{g \in \mathcal{G}} U_g^\dagger U_\Delta U_g \right)^n, \quad (9)$$

with free-evolution $U_\Delta = \mathcal{T} \exp \left(-i \int_0^\Delta H_{tot}(\tau) d\tau \right)$.

By Schur's lemma, the twirling channel $\Pi_{\mathcal{G}}(\cdot)$ acts as a projection and retains only the components of H_{tot} that commute with all elements of the group \mathcal{G} . When the

map $g \rightarrow U_g$ defines an irreducible representation of \mathcal{G} , the projection takes the form [7, 8, 31, 32]

$$\Pi_{\mathcal{G}}(O) = \frac{\text{Tr}(O)}{d} I_d. \quad (10)$$

where d is the dimension of the system Hilbert space. In this special case, the DD procedure completely averages out all nontrivial system operators and the effective system Hamiltonian becomes proportional to the identity. This corresponds to a trivial global phase, meaning that the system dynamics are completely frozen.

When the representation is reducible, the twirling operation projects any operator O onto the multiplicity spaces associated with each irreducible representation. By Maschke's theorem, the system Hilbert space \mathcal{H}_S can be decomposed as

$$\mathcal{H}_S \cong \bigoplus_{\alpha} V_{\alpha} \otimes \mathbb{C}^{m_{\alpha}}, \quad (11)$$

where $\{V_{\alpha}\}$ are inequivalent irreducible representations of dimension d_{α} , and m_{α} denotes the multiplicity with which V_{α} appears in the decomposition. By Schur's lemma, the commutant algebra of $\{U_g\}$ takes the form

$$\bigoplus I_{d_{\alpha} \times d_{\alpha}} \otimes \text{Mat}_{m_{\alpha}}(\mathbb{C}), \quad (12)$$

where $\text{Mat}_{m_{\alpha}}(\mathbb{C})$ denotes the full algebra of $m_{\alpha} \times m_{\alpha}$ complex matrices acting on the multiplicity space. If the characters $\chi_{\alpha}(g)$ of the irreducible representations V_{α} are known, then the action of the twirling operation is

$$\Pi_{\mathcal{G}}(O) \cong \bigoplus_{\alpha} \frac{I_{d_{\alpha} \times d_{\alpha}}}{d_{\alpha}} \otimes \text{Tr}_{V_{\alpha}}(P_{\alpha} O P_{\alpha}), \quad (13)$$

where P_{α} is the orthogonal projector onto the α -th isotypic component, given by

$$P_{\alpha} = \frac{d_{\alpha}}{|G|} \sum_{g \in \mathcal{G}} \chi_{\alpha}^*(g) U_g. \quad (14)$$

In the special case where all irreducible representations appear with multiplicity one (i.e., the decomposition is multiplicity-free), the twirling map simplifies to a projection of O onto each irreducible block

$$\Pi_{\mathcal{G}}(O) = \sum_{\alpha} P_{\alpha} \frac{\text{Tr}(O P_{\alpha})}{d_{\alpha}}. \quad (15)$$

By selecting a group \mathcal{G} whose action on \mathcal{H}_S admits a suitable irreducible decomposition, one can engineer the twirling operation to selectively preserve desired interaction terms in a Hamiltonian. In a later section, we will analyze the commutant algebra of $\{U_g\}$ directly through the framework of error detection codes.

In this work, we restrict ourselves to the analysis of π -pulses generating X, Y, Z , and I gates on a system of N qubits. Consequently, we choose the DD group \mathcal{G} to be a subgroup of the N -qubit Pauli group modulo phases,

i.e. $\mathcal{G} \subseteq \mathcal{P}^N / \{\pm i, \pm 1\}$. The corresponding unitary representation maps each group element $g \in \mathcal{G}$ to its associated standard Pauli operator acting on the system Hilbert space.

To illustrate this formalism, we consider, for example, one cycle of the standard single-qubit XY4 sequence, defined by the unitary time-evolution operator

$$U(T_c) = XU_\Delta YU_\Delta XU_\Delta YU_\Delta, \quad (16)$$

where U_Δ is a single-qubit free evolution operator for a time Δ . This sequence has a DD group \mathcal{G} corresponding to the full single-qubit Pauli group. This can be seen explicitly by expressing the sequence as a product of Pauli operators applied before and after each free evolution period and using Pauli matrix identities ($XY = Z$ and cyclic permutations)

$$U(T_c) \equiv (XU_\Delta X)(ZU_\Delta Z)(YU_\Delta Y)(IU_\Delta I). \quad (17)$$

This decomposition shows that each interval is conjugated by a Pauli operator and the full sequence effectively performs a twirl over the single-qubit Pauli group. Consequently, the XY4 sequence removes all single-qubit terms, leading to a universal suppression of disorder

In bounded-control schemes [30, 31], the requirement of applying arbitrarily strong and instantaneous control pulses $U_{g_{j+1}}U_{g_j}^\dagger$ at discrete times $t = j\Delta$ is relaxed. Instead, the control strategy involves smoothly interpolating between successive group elements, implementing a continuous transition from U_{g_j} to $U_{g_{j+1}}$ over each subinterval. More details on bounded-control can be found in Appendix A.

III. PERMUTATION-INVARIANT DECOUPLING GROUP FROM GRAPH SYMMETRY

In this section, we systematically reformulate and extend the protocols introduced in Refs. [24, 27, 33] using the language of graph theory. This approach enables a more natural description of interactions in the Hamiltonian through hypergraphs and captures system symmetries via quotient graphs. The flowchart of the framework proposed in this work is summarized in Fig. 2.

A. Hypergraph coloring

To describe a general Hamiltonian of N interacting qubits, we introduce the interaction graph $I_{\text{Dev}} = (V_I, E_I)$. The vertex set V_I represents physical qubits. The interaction graph is a hypergraph, where each hyperedge connects a subset of vertices, potentially more than two. A hyperedge $e_i \in E_I$ connecting vertices $(v_{i_1}, \dots, v_{i_N})$ corresponds to a general noise model in which arbitrary Pauli interactions from $\{I, X, Y, Z\}^{\otimes N}$

may jointly act on these qubits, unless otherwise specified. This corresponds to the first step of Fig. 2a. A Pauli string associated with such a hyperedge is called k -local if it has support on exactly k distinct vertices. Therefore, the interaction graph I_{Dev} characterizes a k -local Hamiltonian if and only if all of its hyperedges involve at most k vertices. Under this definition, the Hamiltonian considered in Refs. [24, 27] are two-local and the interaction graph I_{Dev} coincides with the device connectivity graph.

We now generalize the results of Refs. [24, 27] to arbitrary k -local Hamiltonians. In the first-order Magnus expansion given in Eq. (6), a vertex v_i only interacts with other vertices that share a common hyperedge. This motivates a natural vertex coloring of the interaction graph. We assign a distinct color c_i to each vertex $v_i \in V_I$, such that no two vertices $(v_i, v_j) \in E_I$ in a hyperedge share the same color (step 2 of Fig. 2a). We denote this graph coloring as $C[I_{\text{Dev}}]$, and refer to the number of colors used (i.e. the chromatic number) as χ_I .

We remark that general hypergraph coloring problems can be addressed efficiently using well-established graph-coloring algorithms [40]. However, standard graph-coloring algorithms are typically designed for 2-local graphs, where each edge connects exactly two vertices. To apply these algorithms to a hypergraph coloring problem, we formally construct an auxiliary graph by adding an edge between each pair of vertices v_i and v_j that share a hyperedge in I_{Dev} . A proper coloring of this auxiliary graph corresponds to a valid coloring of the original hypergraph.

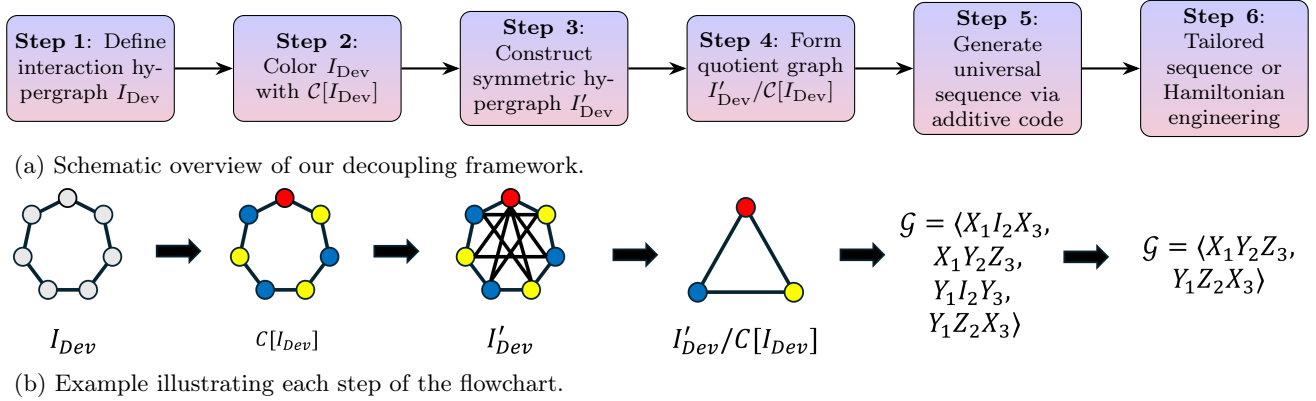
In the next section, we show that the color partition $C[I_{\text{Dev}}]$ respects an underlying graph symmetry. Using this symmetry, the problem of designing a DD sequence for the interaction graph I_{Dev} is significantly simplified.

B. Symmetry and quotient graph

We begin by constructing an expanded graph $I'_{\text{Dev}} = (V_I, E'_I)$ from I_{Dev} such that $I_{\text{Dev}} \subseteq I'_{\text{Dev}}$, and the original coloring $C[I_{\text{Dev}}]$ remains a valid vertex coloring for I'_{Dev} . Because $I_{\text{Dev}} \subseteq I'_{\text{Dev}}$, any DD group \mathcal{G} designed for I'_{Dev} is also valid decoupling group for I_{Dev} .

More precisely, the expanded graph I'_{Dev} is constructed from I_{Dev} and its coloring $C[O_{\text{Dev}}]$ as follows. The graph I'_{Dev} shares the same vertex set $V'_I = V_I$ as I_{Dev} . We traverse the colored interaction graph I_{Dev} and record all tuples $(c_{i_1}, \dots, c_{i_N})$ such that there exists a hyperedge in I_{Dev} connecting vertices with those colors. The new hyperedge set E'_I is then constructed by appending to the original set E_I additional hyperedges of the form $(v_{i_1}, \dots, v_{i_N}) \notin E_I$, where the vertices $(v_{i_1}, \dots, v_{i_N})$ have distinct colors that match one of the recorded color tuples $(c_{i_1}, \dots, c_{i_N})$. This procedure ensures that the color partition $C[I_{\text{Dev}}]$ remains valid for the expanded graph I'_{Dev} , see step 3 of Fig. 2a.

To better illustrate this construction, here we apply it



(b) Example illustrating each step of the flowchart.

FIG. 2: **Framework for constructing efficient dynamical decoupling sequences.** (a) Flowchart of our approach. Starting from an interaction hypergraph, we color it, generate a symmetric variant, and construct its quotient. Additive codes are then used to produce efficient universal sequences, which are tailored to suppress specific Hamiltonian terms. (b) Example of each step in the protocol. We start from a simple 7-qubit loop (step 1) and we color it with a color partition under a nearest-neighbor interaction model (step 2). We then construct a color-preserving symmetric graph connecting all different colors (step 3), that permits to simplify the DD problem by just considering the corresponding quotient graph (step 4). The DD sequence is then constructed by using additive codes, allowing us to construct a universal decoupling group that freezes arbitrary two-local interactions (step 5). We then tailor the sequence for specific qubit architectures (step 6).

to an explicit example. We consider a system of seven qubits arranged in a bilinear array with two-local interactions. Figure 3(a) illustrates the corresponding interaction graph I_{Dev} along with its vertex coloring $C[I_{\text{Dev}}]$. A general Hamiltonian for this system is

$$H = \sum_i \vec{h}_i \cdot \vec{\sigma}_i + \sum_{\langle ij \rangle} \vec{\sigma}_i \cdot A_{ij} \vec{\sigma}_j. \quad (18)$$

where \vec{h}_i are local fields and A_{ij} are real coupling matrices that specify pairwise interactions. For this example, the expanded graph I'_{Dev} constructed from the above procedure is shown in Fig. 3(b).

The expanded graph I'_{Dev} may appear more complex than the original interaction graph I_{Dev} , suggesting that designing a suitable decoupling group \mathcal{G} for I'_{Dev} could be more challenging. However, I'_{Dev} inherits a strong symmetry from the color partition $C[I_{\text{Dev}}]$. In particular, I'_{Dev} is invariant under permutations of vertices that share the same color, a symmetry we (with a slight abuse of notation) also denote by $C[I_{\text{Dev}}]$. This invariance significantly simplifies the construction of the DD group: it implies that it suffices to consider DD groups \mathcal{G} that themselves respect the symmetry $C[I_{\text{Dev}}]$ [41]. Practically, this means applying identical control pulses to all qubits within the same color class.

As a complementary view on this symmetry, rather than directly working with the symmetric decoupling group \mathcal{G} , we can instead analyze the quotient graph $I'_{\text{Dev}}/C[I_{\text{Dev}}]$. The quotient graph $I'_{\text{Dev}}/C[I_{\text{Dev}}]$ is formed by collapsing all vertices $v_i \in V'_I$ with the same color c_i into a single super-vertex $c_i \in V'_I/C[I_{\text{Dev}}]$ in the quotient graph. A hyperedge $(c_{i_1}, \dots, c_{i_N})$ exists in the quotient graph if and only if there is at least one hyperedge

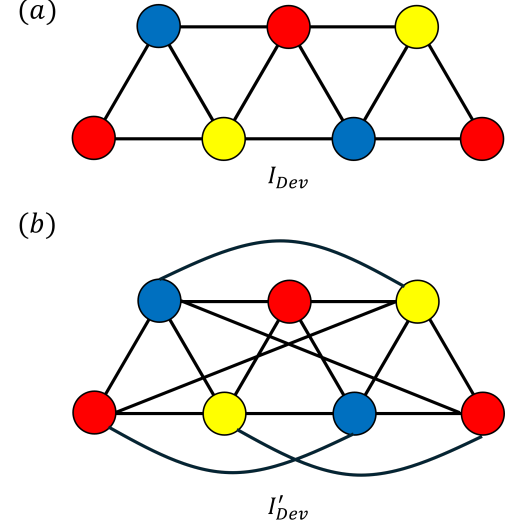


FIG. 3: **Colored bilinear array graph.** (a) Interaction graph I_{Dev} of 7 physical qubits with two-local interactions arranged in a bilinear array, along with the minimal color partition $C[I_{\text{Dev}}]$. (b) Expanded interaction graph I'_{Dev} constructed from I_{Dev} and $C[I_{\text{Dev}}]$.

$(v_{i_1}, \dots, v_{i_N}) \in E'_I$, such that the vertices V_{i_j} are colored c_{i_j} respectively. Figure 4 illustrates this transformation from the expanded graph I'_{Dev} (shown in Fig. 3) to its corresponding quotient graph $I'_{\text{Dev}}/C[I_{\text{Dev}}]$. We emphasize that the same quotient graph also captures different topologies, including the ring topology in Fig. 2.

It follows directly that if $\Pi_{\mathcal{G}}$ is a DD sequence that universally suppresses all interactions in the quotient graph $I'_{\text{Dev}}/C[I_{\text{Dev}}]$, then this sequence can be lifted to a valid

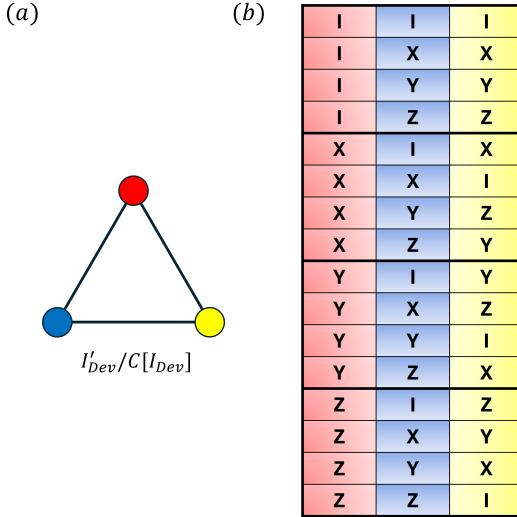


FIG. 4: **Dynamical decoupling from orthogonal arrays.** (a) The quotient graph $I'_\text{Dev}/C[I_\text{Dev}]$ formed by collapsing all physical qubits of the same color in I'_Dev into a single equivalence class. (b) The orthogonal array $\text{OA}(L = 16, \chi_I = 3, S = 4, k = 2)$ which generates a universal DD sequence for two-local Hamiltonians defined by the quotient graph $I'_\text{Dev}/C[I_\text{Dev}]$. Each column is colored according to the associated color qubits c_i .

decoupling sequence for the expanded graph I'_Dev , and consequently on the interaction graph I_Dev . The lifting procedure consists of applying the same control pulses in parallel to all vertices in I'_Dev that share the same color c_i . This approach is valid for both bang-bang and bounded-strength control schemes.

We note that the explicit construction of the expanded interaction graph I'_Dev in principle is not required to design the DD group. Rather, it provides a conceptual tool that reveals the underlying symmetry structure of the colored interaction graph. The expanded graph also provides a key general insight, namely any two interaction graphs that share the same expanded graph I'_Dev can be universally decoupled using the same DD group \mathcal{G} , see the examples in Figs. 2 and 3. In fact, an even stronger statement holds: if two interaction graphs share the same quotient graph $I'_\text{Dev}/C[I_\text{Dev}]$ and interaction models, they admit the same DD group capable of universally suppressing their system interactions.

In the following section, we demonstrate how to obtain time-efficient decoupling groups for the quotient graph $I'_\text{Dev}/C[G_\text{Dev}]$ using constructions from classical coding theory.

IV. TIME-EFFICIENT DECOUPLING GROUP FROM CLASSICAL ADDITIVE CODES

We now discuss how to construct time-efficient DD groups using classical additive codes. Specifically, we es-

tablish a connection between DD sequences and classical additive codes by using orthogonal arrays [30, 32]. As a result, we can analyze the properties of a DD group in terms of its generators, in analogy to how stabilizer codes are characterized by their stabilizer generators [42].

A. Orthogonal arrays and dynamical decoupling

Time-efficient DD sequences can be constructed using combinatorial design objects. For example, Ref. [27] employs Hadamard matrices to construct decoupling sequences for two-local Hamiltonians. We generalize this approach to arbitrary k -local Hamiltonians by using more general combinatorial structures known as orthogonal arrays [30, 32, 43]. In the following analysis, we consider the worst-case scenario where all possible k -local interactions between the colored qubits c_i are present in the quotient graph $I'_\text{Dev}/C[I_\text{Dev}]$.

An orthogonal array $\text{OA}(L, \chi_I, S, k)$ is an $L \times \chi_I$ array with entries taken from a finite set S and strength k , such that every possible k -tuple from $S^{\otimes k}$ appears uniformly across any choice of k columns [44]. In this work, we restrict ourselves to the set $S = \{I, X, Y, Z\}$ of single-qubit Pauli operators. Each column of the orthogonal array is associated with a colored qubit c_i , and each row defines a group element in the DD group \mathcal{G} . If the noise model is biased along a specific axis of the Bloch sphere (e.g. the Z -axis for pure dephasing) or if we want to maintain certain interactions (e.g. XX interactions), we can reduce the required size L of the orthogonal array by selecting a smaller set (e.g. $S = \{I, X\}$) instead of the full single-qubit Pauli group. We remark that for any choice of parameters χ_I , S , and strength k , there always exists an orthogonal array whose length L is determined by these parameters [44].

In Fig. 4, we show the explicit orthogonal array $\text{OA}(L = 16, \chi_I = 3, |S| = 4, k = 2)$, which generates a universal decoupling sequence for two-local Hamiltonians defined on the quotient graph $I'_\text{Dev}/C[I_\text{Dev}]$ [45]. One can verify that for any pair of columns, the rows of the OA exhaustively span all combinations of $\{I, X, Y, Z\}^{\otimes 2}$ exactly once. Moreover, each Pauli operator appears exactly four times in every column, ensuring balanced coverage and uniformity.

By construction, the action of the DD group \mathcal{G} derived from an OA with strength k implements a group twirl over the k -fold Pauli group $\{I, X, Y, Z\}^{\otimes k}$ on any subset of k colored qubits. As a consequence, all k -local interaction terms are dynamically canceled, following directly from Schur's lemma [Eq. (10)]. Furthermore, all interactions with support on less than k colored qubits are also canceled as a consequence of this construction. Therefore, to universally decouple all k -local interactions on the quotient graph $I'_\text{Dev}/C[I_\text{Dev}]$, it suffices to construct the orthogonal array $\text{OA}(L, \chi_I, S, k)$.

We note that there is a comprehensive online library cataloging efficient orthogonal arrays across a wide range

of parameters [45]. In the next section, we describe how to construct length-efficient orthogonal arrays by leveraging their connection to classical error-correcting codes. Since classical codes are extensively studied, we can utilize well-established classical codes to obtain time-efficient DD sequences suppressing arbitrary k -local interactions [30].

B. Orthogonal array and classical additive codes

The connection between orthogonal arrays and classical linear codes is well established [44, 46]. In this work, we focus on the single-qubit Pauli group modulo global phases, which admits a natural isomorphism to the finite field \mathbb{F}_4 . A finite field \mathbb{F}_q is a set containing q elements in which addition, subtraction, multiplication, and division (except by zero) are all well-defined and satisfy the field axioms. The isomorphism between Pauli group (modulo phase) and \mathbb{F}_4 is defined by the correspondence

$$I \rightarrow 0, X \rightarrow 1, Z \rightarrow \omega, Y \rightarrow 1 + \omega, \quad (19)$$

where ω is a primitive element of \mathbb{F}_4 satisfying $\omega^2 = \omega + 1$. The addition and multiplication tables for \mathbb{F}_4 are

+	0	1	ω	$1 + \omega$
0	0	1	ω	$1 + \omega$
1	1	0	$1 + \omega$	ω
ω	ω	$1 + \omega$	0	1
$1 + \omega$	$1 + \omega$	ω	1	0

(20)

and

\times	0	1	ω	$1 + \omega$
0	0	0	0	0
1	0	1	ω	$1 + \omega$
ω	0	ω	$1 + \omega$	1
$1 + \omega$	0	$1 + \omega$	1	ω

(21)

This correspondence allows us to represent Pauli operators algebraically as elements of \mathbb{F}_4 , providing a convenient framework for constructing orthogonal arrays from quaternary codes. Furthermore, when the noise is biased (e.g., dephasing along the Z -axis), we may restrict to a subset of the Pauli group, in which case classical codes over the binary field \mathbb{F}_2 become relevant.

We consider here classical additive codes, which, as we will show in Section IV C, provide a natural framework for interpreting DD as an error detection code. An additive code \mathcal{C} is a subset of \mathbb{F}_q^n (a vector of length n in which its entries are from \mathbb{F}_q) that is closed under addition. While every linear code is an additive code, the converse is not true: additive codes are not necessarily closed under scalar multiplication unless the field is \mathbb{F}_2 .

We characterize the code \mathcal{C} by the set of parameters $(n, |\mathcal{C}|, d)_q$, where n is the length of the codeword, $|\mathcal{C}|$ is the number of distinct code words, and d is the code distance. The entries of each codeword are elements of the finite field \mathbb{F}_q . The distance d is defined as the minimum

Hamming distance between any two distinct codewords $\mathbf{u}, \mathbf{v} \in \mathcal{C}$. Since \mathcal{C} is closed under addition, this is equivalent to the minimum Hamming weight of any nonzero codeword

$$d = \min_{\mathbf{u} \neq 0 \in \mathcal{C}} \text{wt}_H(\mathbf{u}). \quad (22)$$

The vector space \mathbb{F}_4^n can be endowed with an inner product $\langle \cdot, \cdot \rangle$. A natural choice for additive codes is the trace Hermitian inner product [47], defined as

$$\langle \mathbf{u}, \mathbf{v} \rangle_{\text{tr}} = \sum_i (\mathbf{u}_i \mathbf{v}_i^2 + \mathbf{v}_i \mathbf{u}_i^2). \quad (23)$$

Under the mapping between single-qubit Pauli operators and elements of \mathbb{F}_4 given in Eq. (19), this inner product directly encodes the commutation relations of Pauli operators, that is, it evaluates to zero if the corresponding Pauli operators commute and to one if they anticommute.

Using the trace Hermitian inner product, we define the dual code \mathcal{C}^\perp of an additive code \mathcal{C} as

$$\mathcal{C}^\perp = \{ \mathbf{v} \in \mathbb{F}_q^n \mid \langle \mathbf{u}, \mathbf{v} \rangle_{\text{tr}} = 0, \quad \forall \mathbf{u} \in \mathcal{C} \}. \quad (24)$$

We denote the minimum distance of the dual code by d^\perp . Importantly, the dual code \mathcal{C}^\perp is always an additive code, regardless of whether \mathcal{C} is linear or additive. However, it is known that if \mathcal{C} is an additive code of size $|\mathcal{C}| = 2^l$ for some positive integer $l \leq 2n$, then its dual code has size $|\mathcal{C}^\perp| = 2^{2n-l}$. This follows from the fact that \mathbb{F}_4^n is isomorphic to \mathbb{F}_2^{2n} under addition.

A seminal result by Delsarte [46] establishes a fundamental connection between orthogonal arrays and classical codes:

Theorem IV.1. *If \mathcal{C} is a code $(n, |\mathcal{C}|, d)_q$ with dual distance d^\perp , then the codewords of \mathcal{C} form the rows of an OA($|\mathcal{C}|, n, q, d^\perp - 1$) with entries from \mathbb{F}_q . Conversely, the rows of a linear OA($|\mathcal{C}|, n, q, k$) over \mathbb{F}_q form a linear code $(n, |\mathcal{C}|, d)_q$ over \mathbb{F}_q with dual distance $d^\perp \geq k + 1$. If the orthogonal array has strength k but not $k + 1$, d^\perp is precisely $k + 1$.*

This theorem highlights the direct connection between the strength of an OA and the dual distance d^\perp of the code \mathcal{C} . Consequently, to construct an OA of strength k , corresponding to a universal DD sequence that suppresses k -local interactions in the original Hamiltonian, it suffices to use the dual code \mathcal{C}^\perp of a code \mathcal{C} with distance $d = k + 1$.

In Ref. [30], Bose–Chaudhuri–Hocquenghem (BCH) codes [48, 49] were used to construct efficient universal DD sequences for k -local Hamiltonians acting on physical qubits. By applying their construction to the quotient graph $I'_{\text{Dev}}/C[I_{\text{Dev}}]$ and assuming 1-local control Hamiltonians, we find that the length L of a single DD cycle required to universally decouple k -local Hamiltonians scales as

$$O(\chi_I^{k-1}) \quad (25)$$

for bang-bang control, and as

$$O(\chi_I^{k-1} \log \chi_I) \quad (26)$$

for bounded-strength control (see Appendix A).

In Section V, we will present different constructions based on alternative classical codes that generates more time-efficient decoupling groups for 2-local and 3-local Hamiltonians. While the asymptotic scaling remains the same as in Eqs. (25) and (26), our constructions enable improved constant prefactors compared to those based on BCH codes for the 2-local and 3-local cases.

In the next section, we tighten the connection between DD and error detection codes by drawing an analogy to quantum stabilizer codes. With this viewpoint, if the structure of the noise model is known, or if the goal is to engineer a specific Hamiltonian, it becomes possible to design significantly more time-efficient DD sequences tailored to the problem.

C. Dynamical decoupling as error detection codes

Historically, self-dual additive codes over \mathbb{F}_4 (i.e., $\mathcal{C} = \mathcal{C}^\perp$) have played a central role in the construction of stabilizer quantum error-correcting codes [42, 47, 50, 51]. Many properties of stabilizer codes can be analyzed through their stabilizer generators. Similarly, in our setting, we will study the properties of the DD sequence through the generators of the associated additive classical code.

From the definition of the dual code \mathcal{C}^\perp in Eq. (24), it follows that Pauli strings corresponding to codewords in \mathcal{C}^\perp remain invariant under the decoupling sequence generated by \mathcal{C} . In fact, \mathcal{C}^\perp defines the entire invariant subspace of the decoupling sequence. Consequently, to determine whether an interaction is suppressed by the decoupling sequence, one only needs to check whether the associated codeword lies in \mathcal{C}^\perp . At first glance, this may appear computationally expensive because it requires checking the trace Hermitian inner product against all codewords in \mathcal{C} . However, it is not necessary to check the entire code. Instead, it is sufficient to compute the inner products with respect to the generators of \mathcal{C} , which fully characterize the code.

Because \mathcal{C} is an additive code, it is generated by a finite set of independent generators $\Gamma = \{\gamma_1, \dots, \gamma_m\}$, where $|\Gamma| = \log_2 |\mathcal{C}|$. Importantly, if a vector $\mathbf{u} \in \mathbb{F}_4^n$ anticommutes with at least one of the generators γ_i , then the Pauli string associated with \mathbf{u} will be eliminated by the decoupling sequence generated from the code \mathcal{C} [21].

This can be seen explicitly through a simple example. Suppose \mathcal{C} , and equivalently the DD group \mathcal{G} , has two generators γ_1 and γ_2 . The DD group is then

$$\{I, \gamma_1, \gamma_2, \gamma_1\gamma_2\}. \quad (27)$$

We assume without loss of generality that \mathbf{u} anticommutes with γ_1 but commutes with γ_2 . Under conjugation by the elements of \mathcal{G} , the sign of the Pauli string

corresponding to \mathbf{u} evolves as

$$\{+1, -1, +1, -1\}. \quad (28)$$

When twirling over the group \mathcal{G} , all these contributions cancel out, and the corresponding interaction is completely suppressed by the decoupling sequence. The generalization to an arbitrary set of generators Γ follows directly from the same principle: if \mathbf{u} anticommutes with any generator in Γ , then averaging over the decoupling group results in the complete cancellation of the corresponding Pauli term.

We have shown that DD sequences constructed from additive classical codes behave analogously to quantum stabilizer codes. However, we emphasize two key differences. First, unlike quantum stabilizer codes, we do not require the generators of the decoupling group \mathcal{G} to commute with each other. Second, in the context of dynamical decoupling, there is no active "correction" step. Instead, the twirling procedure passively removes all components of the Hamiltonian that anticommute with at least one of the generators of \mathcal{G} . In this sense, the role of the decoupling sequence is similar to that of an *error detection code* rather than an error correction code.

The connection between designing decoupling sequences and designing error detection codes is a key insight of our work. Specifically, if the dominant residual interactions in the system are known, we can forego a universal decoupling group \mathcal{G} , which suppresses all interactions, and instead remove certain generators from \mathcal{G} while still detecting the dominant residual terms [20]. The resulting DD sequence becomes significantly more time-efficient. We will make extensive use of this idea in Sections VA and VB, where we tailor our general method to specific cases.

As an example, the orthogonal array presented in Fig. 4 that universally decouples all 2-local interactions is generated by the DD group

$$\mathcal{G} = \langle X_1 I_2 X_3, X_1 Y_2 Z_3, Y_1 I_2 Y_3, Y_1 Z_2 X_3 \rangle \quad (29)$$

However, if we know that the residual two-qubit interactions are restricted to terms of the form $X_i X_j, Y_i Y_j$, or $Z_i Z_j$, as is the case e.g. in spin qubits [52–55], the reduced decoupling group

$$\mathcal{G}_{\text{red}} = \langle X_1 Y_2 Z_3, Y_1 Z_2 X_3 \rangle \quad (30)$$

still detects all the relevant interactions. Explicitly, the elements of \mathcal{G}_{red} are

$$\mathcal{G}_{\text{red}} = \{I_1 I_2 I_3, X_1 Y_2 Z_3, Y_1 Z_2 X_3, Z_1 X_2 Y_3\}. \quad (31)$$

We note that this group corresponds to running the standard XY4 sequence in parallel on all three qubits, with the XY4 cycles on the second and third qubits being cyclically shifted relative to each other. Moreover, the reduced group \mathcal{G}_{red} universally decouples all single-qubit terms. As a result, the DD sequence requires only $2^2 = 4$

time steps instead of $2^4 = 16$, achieving a fourfold reduction in cycle length.

Another interesting consequence of our error-detection perspective is that it enables the construction of decoupling sequences that selectively suppress certain interactions while preserving others [24, 56]. For instance, in systems where anisotropic exchange interactions arise, such as spin qubits with strong spin-orbit coupling [56–58], the decoupling sequence generated by Eq. (30) preserve specific components of the antisymmetric Dzyaloshinskii–Moriya (DM) interaction. In particular, it maintains terms of the form:

$$\{X_1Y_2, Y_1Z_2, Y_2Z_3, Z_2X_3, X_1Z_3, Y_1X_3\}. \quad (32)$$

By alternating between DD sequences derived from \mathcal{G}_{red} and suitably permuted variants of it, one can fully preserve the complete DM interaction, thus enabling new possibilities for quantum simulation [59, 60].

We will discuss more examples of sequences simulating certain Hamiltonians in Section V C. In the next section, we introduce a search algorithm to construct selective DD sequences.

Finally, we remark that if one uses a quantum stabilizer code (i.e a self-dual additive code) to construct a DD sequence in parallel with employing the same code for active error correction, it is possible to improve the overall code threshold by suppressing high-weight errors. This idea was explored in Refs. [20, 21], where the authors designed decoupling sequences based on the stabilizers and logical operators of a quantum code to suppress high-weight error strings. We do not directly compare our sequences with those proposed in Refs. [20, 21], as they serve fundamentally different purposes. The sequences in that work scale exponentially with the quantum code (system) size but are used alongside a quantum error-correcting code, such that errors that accumulate due to the long sequence length can be actively corrected. In contrast, our sequences are designed to protect bare physical qubits without additional quantum error correction. An interesting direction for future work is to combine our approach with that of Refs. [20, 21], to explore trade-offs between sequence length and robustness against errors in the presence of a quantum code.

D. Selective DD sequences

We now apply our formalism to selectively cancel only particular interactions, rather than to completely decouple the system from the environment or suppress all residual interactions. To do so, we assume that the system Hamiltonian H_S can be decomposed into two parts:

$$H_S = H_S^{\parallel} + H_S^{\perp}, \quad (33)$$

where H_S^{\parallel} contains the interaction terms we wish to preserve and H_S^{\perp} contains the terms we aim to suppress. This task is particularly relevant for applications such

as Hamiltonian simulation, where it is desirable to selectively engineer specific interactions [29].

Based on the connection between DD sequences and error-detection codes, we can construct a simple algorithm that finds the DD group performing this task. Our method explicitly searches for generators of the DD group that suppresses the undesired terms in H_S^{\perp} while preserving the desired terms in H_S^{\parallel} .

As a first step, we identify a set of generators that commute with all terms in H_S^{\parallel} . This is efficiently achieved by representing each Pauli string in H_S^{\parallel} as a binary vector in \mathbb{F}_2^{2n} via the mapping

$$\vec{P} = \left(\prod_{i=1}^n X_i^{x_i} Z_i^{z_i} \right) \rightarrow (\vec{x} \mid \vec{z})^T \quad \text{with } \vec{x}, \vec{z} \in \mathbb{F}_2^n. \quad (34)$$

In this representation, the commutation relation between two Pauli strings \mathbf{u} and \mathbf{v} is determined by their symplectic inner product

$$\mathbf{u}^T \Omega \mathbf{v}, \quad \text{where} \quad \Omega = \begin{pmatrix} 0_{n \times n} & I_{n \times n} \\ I_{n \times n} & 0_{n \times n} \end{pmatrix}. \quad (35)$$

The two strings commute if and only if this inner product is zero.

Let $\{\mathbf{h}_i^{\parallel}\}_{i=1}^M$ be the binary vector representations of the Pauli strings in H_S^{\parallel} , where M is the number of strings. The set of binary vectors (and corresponding Pauli strings) that commute with all elements of H_S^{\parallel} forms the null space of the matrix

$$\begin{pmatrix} (\mathbf{h}_1^{\parallel})^T \\ \vdots \\ (\mathbf{h}_M^{\parallel})^T \end{pmatrix} \Omega. \quad (36)$$

This null space can be efficiently computed via standard Gaussian elimination over \mathbb{F}_2 .

Let $\{\mathbf{n}_i\}$ denote the binary vector generators of the null space from Eq. (36). To construct a minimal decoupling sequence that suppresses H_S^{\perp} , we form a bipartite graph whose two partitions consist of the null space generators $\{\mathbf{n}_i\}$ and the Pauli terms $\{\mathbf{h}_i^{\perp}\}$ from H_S^{\perp} . An edge is drawn between \mathbf{n}_i and \mathbf{h}_j^{\perp} if and only if they anti-commute, i.e.

$$\mathbf{n}_i^T \Omega \mathbf{h}_j^{\perp} = 1 \pmod{2}. \quad (37)$$

Constructing this graph requires computing all pairwise symplectic inner products, with a total complexity of $O(|\{\mathbf{n}_i\}| |\{\mathbf{h}_i^{\perp}\}|)$.

Given the bipartite graph, we numerically identify the minimal set of generators $\{\mathbf{n}_i\}$ that preserves H_S^{\parallel} while decoupling H_S^{\perp} . This reduces to the classical minimum set cover problem: finding the smallest subset of $\{\mathbf{n}_i\}$ such that every \mathbf{h}_i^{\perp} anticommutes with at least one selected generator. While set cover is generally a NP-hard problem, this problem remains tractable in simple cases,

where we assume the chromatic number χ_I is small, an assumption typically valid for planar devices with short range interactions.

We emphasize that this algorithm is primarily a proof of concept rather than a fully optimized solution. Nonetheless, it shows that the error-detection perspective can drastically reduce the search space by focusing only on the generators of the decoupling group instead of the entire sequence, generally enabling a more efficient and automated construction of tailored decoupling sequences. This viewpoint could also potentially benefit machine learning-based approaches to decoupling design, as explored in recent work [33, 34].

V. APPLICATIONS TO QUANTUM COMPUTING

In the previous section, we linked the problem of designing time-efficient DD sequences for arbitrary k -local Hamiltonians to classical error detection codes. Here, we explicitly construct DD sequences for 2-local and 3-local Hamiltonians, tailored to superconducting and spin qubits, using known constructions of classical additive codes. As an example of Hamiltonian engineering, we also introduce a sequence that enables the simulation of the Kitaev's honeycomb model in spin qubit platforms.

A. Residual ZZ and ZZZ coupling in superconducting qubits

1. Suppressing ZZZ coupling

In superconducting platforms, suppressing residual ZZ and ZZZ couplings between neighboring qubits is a key challenge for scalability, as these interactions are a major source of coherent errors [61–63].

In this section, we show that by combining the graph coloring procedure introduced earlier with binary Reed–Muller codes, one can construct efficient DD sequences. Specifically, we introduce a bang-bang control sequence with circuit depth scaling as $O(\chi_I)$. In Appendix B, we extend this result to bounded-strength control, yielding a DD sequence with depth scaling as $O(\chi_I \log \chi_I)$.

As a concrete example, Fig. 5(a) and Fig. 5(b) show the color partitions using $\chi_I = 6$ for the heavy-hex lattice and the square lattice, used by IBM [64] and Google [65] respectively. In this section, we assume a noise model in which each qubit is subject to both dephasing and relaxation, along with residual ZZ interactions between neighboring qubits and ZZZ interactions across any three consecutive qubits. The presented color partitions also apply when considering residual ZZ interactions between both nearest and next-nearest neighbors. Fig. 5(c) shows the corresponding quotient graph induced by the color partition. We emphasize that both

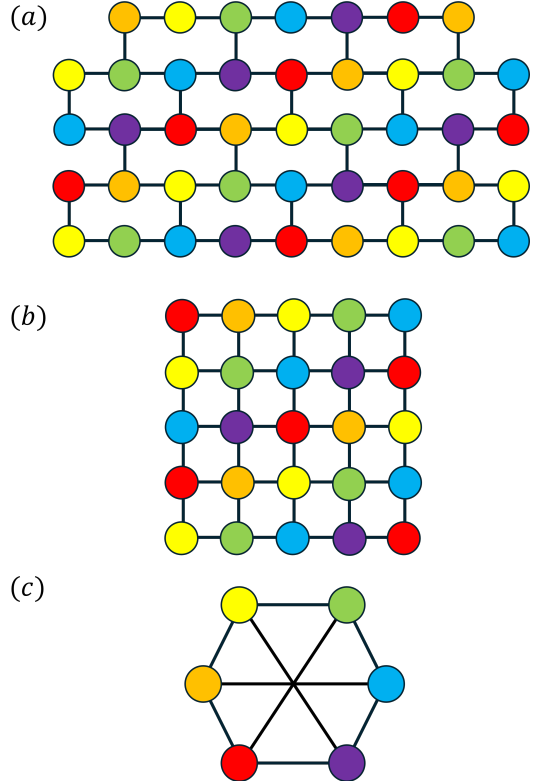


FIG. 5: **Colored graphs of common superconducting qubit architectures.** We assume a noise model where each qubit experiences both dephasing (Z errors) and relaxation (X and Y errors), along with residual ZZ interactions between neighbors and ZZZ interactions among any three consecutive qubits. The colorings also apply when residual ZZ interactions extend to next-nearest neighbors. (a) Heavy-hex lattice with $\chi_I = 6$ colors. (b) Square lattice with $\chi_I = 6$ colors. (c) The resulting quotient graph is identical for both architectures.

the heavy-hex and square lattices yield the same quotient graph under this partitioning. In the following, we briefly review the Reed–Muller code and outline how to construct tailored DD sequences for superconducting qubits based on it.

The Reed–Muller code is one of the oldest and simplest families of linear binary codes with well-understood parameters and dual structure [66]. A Reed–Muller code $RM(r, m)$ is a binary code with parameters

$$(n, |\mathcal{C}|, d)_q = (2^m, 2^{\sum_{i=0}^r \binom{m}{i}}, 2^{m-r})_2 \quad (38)$$

The dual of $RM(r, m)$ is also a Reed–Muller code, specifically $RM(m-r-1, m)$. The generators $\{\gamma_i\}$ of the Reed–Muller code $RM(r, m)$ can be constructed using Boolean polynomials of degree at most r . Each generator γ_i corresponds to a monomial of the form

$$\gamma_i \rightarrow f_{\gamma_i}(\mathbf{x}) = x_{i_1} x_{i_2} \dots x_{i_s}, \quad (39)$$

where $\mathbf{x} = (x_1, \dots, x_m) \in \mathbb{F}_2^m$, $0 \leq s \leq r$, and the total

degree of f_{g_i} is at most r . There are exactly

$$\sum_{i=0}^r \binom{m}{i} \quad (40)$$

of such linearly independent monomials, corresponding to the dimension of the code. Each generator γ_i is a binary vector of length 2^m obtained by evaluating the associated polynomial $f_{\gamma_i}(\mathbf{x})$ at all 2^m possible input $\mathbf{x} \in \mathbb{F}_2^m$.

We will use the Reed-Muller code $\mathcal{C} = \text{RM}(1, m)$ to construct our DD sequence. The dual code of $\text{RM}(1, m)$ is $\mathcal{C}^\perp = \text{RM}(m-2, m)$, consequently, it has the dual distance

$$d^\perp = 2^{m-(m-2)} = 4. \quad (41)$$

If we replace each codeword in \mathcal{C} by substituting 0 with the identity I and 1 with X , then Theorem IV.1 ensures that the resulting DD sequence removes all Z -type interactions with weight up to $d^\perp - 1 = 3$.

The generators of $\text{RM}(1, m)$ correspond to all linear Boolean functions over \mathbb{F}_2^m , i.e., the constant function $f_{\gamma_0} = 1$ and the monomials $f_{\gamma_i} = x_i$ with $i = 1, \dots, m$. As an example, Table Ia lists the generators of $\text{RM}(1, 3)$ as rows, corresponding to the chromatic number $\chi_I = 2^3 = 8$. The generator γ_0 (first row) associated with the constant function $f_{\gamma_0} = 1$ can detect all single-qubit Z_i terms as well as any three-qubit $Z_i Z_j Z_k$ terms. In addition, the other generators $\gamma_{i \geq 1}$ detect two-qubit $Z_i Z_j$ interactions between qubits with distinct colors. Importantly, since the heavy-hex and square lattices in Fig. 5 require only $\chi_I = 6$ colors, the DD sequences derived from Table Ia is directly applicable to these architectures.

The DD sequence constructed from the $\text{RM}(1, m)$ code using the mapping $0 \rightarrow I$ and $1 \rightarrow X$ can only suppresses Z -type interactions. However, to universally suppress all single-qubit terms in addition to residual $Z_i Z_j$ and $Z_i Z_j Z_k$ couplings, a simple modification suffices. The key idea is that the mapping can be generalized by assign 0 to I or Z , and 1 to either X or Y . The result decoupling sequence still removes all Z -type interactions of weight up to three.

To universally decouple single-qubit terms, we require that for each color class the support of the generators must include at least two distinct Pauli operators from $\{X, Y, Z\}$. In other words, each column in Table Ia must contain at least two different Pauli matrices. This condition can always be satisfied for the generators of $\text{RM}(1, m)$ by appropriately applying the substitution rule discussed above. Table Ib provides an example of this modified substitution applied to Table Ia. Consequently, the length L of the decoupling sequence constructed based on the Reed-Muller codes is given by

$$L = 2^{\lceil \log_2(\chi_I) \rceil + 1} \sim O(\chi_I). \quad (42)$$

In practical terms, this means that for the near-term architectures shown in Fig. 5, a tailored bang-bang decoupling sequence of length $L = 16$ is sufficient to protect

C_1	C_2	C_3	C_4	C_5	C_6	C_7	C_8
1	1	1	1	1	1	1	1
1	1	1	1	0	0	0	0
1	1	0	0	1	1	0	0
1	0	1	0	1	0	1	0

(a) Binary generator matrix of $\text{RM}(1, 3)$.

C_1	C_2	C_3	C_4	C_5	C_6	C_7	C_8
X	X	X	X	X	X	X	X
X	X	X	X	Z	Z	Z	Z
X	X	I	I	X	X	I	I
Y	Z	Y	Z	Y	Z	Y	Z

(b) Universal modified generator with Pauli substitutions.

C_1	C_2	C_3	C_4	C_5	C_6	C_7
X	X	X	X	Z	Z	Z
X	X	I	I	X	X	I
Y	Z	Y	Z	Y	Z	Y

(c) Punctured universal modified generator after removing C_8 .

TABLE I: **Suppressing ZZ and ZZZ interactions.** Summary of the generator matrices based on the Reed-Muller $\text{RM}(1, 3)$ code. (a) Binary generator. (b) Universal modified generator with Pauli substitutions for universal decoupling. (c) Punctured version optimized for two-body interactions with one fewer color.

superconducting qubit systems against interactions up to third order. In contrast, as we will show later, using a universal (non-tailored) DD sequence that suppresses all third-order interactions requires a significantly longer sequence of length $L = 64$, a fourfold increase.

2. Tailored sequence to only ZZ couplings

Our DD sequence based on Reed-Muller codes can universally suppress single-qubit terms, as well as two-qubit $Z_i Z_j$ and three-qubit $Z_i Z_j Z_k$ interactions. However, if three-qubit interactions are negligible or absent, we can improve further the time-efficiency of the sequence. This improvement originates from two factors. First, restricting to two-body interactions reduces the chromatic number χ_I of the interaction graph. Second, we can drop one generator from the $\text{RM}(1, m)$ code, effectively halving the length of the decoupling sequence.

The generator we remove is γ_0 which, as previously discussed, detects all weight-three Z -type terms. As a consequence, the final color C_{2^m} (corresponding to the last column of Table Ib) can no longer detect single-qubit Z terms. Therefore, we must also remove this color. This procedure is equivalent to constructing a punctured Reed-Muller code. However, since we also discard γ_0 , the resulting code is a modified punctured $\text{RM}(1, m)$ code with dual distance $d^\perp = 3$ instead of $d^\perp = 4$. Conse-

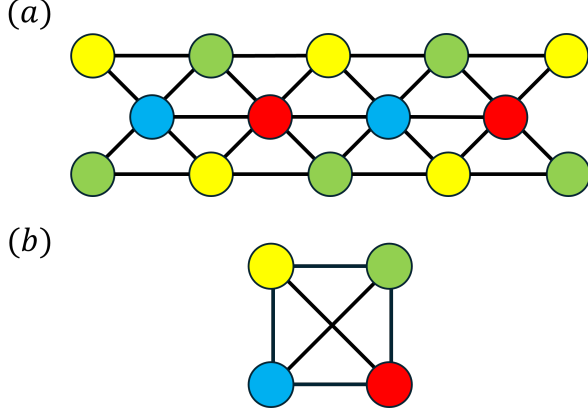


FIG. 6: Colored trilinear array architecture in the spin-qubit platform. We assume a noise model where each qubit undergoes both dephasing and relaxation, with Heisenberg exchange between neighbors and scalar chirality interactions among any three qubits forming a triangle. (a) The color partition $C[I_{\text{Dev}}]$ uses $\chi_I = 4$ colors, tailored to this interaction model. (b) The resulting quotient graph is a square with diagonal links.

quently, the length of the DD sequence is

$$L = 2^{\lceil \log_2(\chi_I + 1) \rceil} \sim O(\chi_I). \quad (43)$$

The resulting decoupling sequence universally suppresses single-qubit terms and two-qubit $Z_i Z_j$ interactions, while requiring one fewer generator at the cost of one fewer color. In Table Ic, we present the generators of such decoupling sequence generated from Table Ib by removing the first row and the last column. This modified punctured RM(1, m) construction is, up to minor adjustments, equivalent to the single-axis Hadamard construction introduced in Ref. [27].

This means that to protect superconducting qubit systems with the architecture shown in Fig. 5 against both nearest-neighbor and next-nearest-neighbor ZZ couplings, a tailored bang-bang DD sequence of length $L = 8$ suffices. In contrast, as we will show later, a universal (non-tailored) DD sequence that suppresses all interactions up to the same order requires a significantly longer sequence of length $L = 32$, again a fourfold increase.

In this section, we have shown how to construct tailored bang-bang DD sequences for removing residual interactions in superconducting qubits by using binary Reed–Muller codes. In Appendix B, we extend this construction to bounded-strength control sequences. In the next section, we turn to the spin-qubit platform and introduce tailored decoupling sequences based on quaternary codes.

B. Exchange interactions in spin qubits

Dense spin-qubit architectures are challenged by residual exchange interaction [56, 57, 67] that cannot be completely turned off. The dominant residual interactions for system with small spin-orbit interaction are the two-qubit Heisenberg exchange interactions

$$\sigma_i \cdot \sigma_j, \quad (44)$$

and the scalar chirality interaction [68] (for perpendicular magnetic fields)

$$\sigma_i \cdot (\sigma_j \times \sigma_k). \quad (45)$$

The class of three-local Hamiltonians is particularly important, as it enables the implementation of single-step, high-fidelity three-qubit gates [56, 69, 70]. As a concrete example, we consider a trilinear array architecture [71] designed to support such gates, as illustrated in Fig. 6(a) [56]. We assume a noise model in which each qubit experiences both dephasing and relaxation, along with Heisenberg exchange interactions between neighboring qubits and scalar chirality interactions among any trio forming a triangle. Under this model, the array admits a coloring with $\chi_I = 4$ colors. The resulting quotient graph is shown in Fig. 6(b).

To construct a tailored DD sequence eliminating all interactions up to weight three, we can generate an orthogonal array by using the projective geometry code \mathcal{C} and its dual (also known as the simplex code) as \mathcal{C}^\perp . The simplex code is chosen because it enables the large number of colors χ_I with minimal number of generators, resulting in a highly time-efficient sequence.

This section is organized as follows. We begin by briefly reviewing the construction of linear and additive codes based on projective geometry with distances $d = 3$ and $d = 4$. We then show how to modify these codes to tailor them to the spin-qubit platform.

1. Linear projective geometry code

A projective geometry space $\text{PG}(n, q)$ is the set of equivalence classes of the vector space $\mathbb{F}_q^{n+1}/\{\mathbf{0}\}$ in which two vectors $\mathbf{u}, \mathbf{v} \in \mathbb{F}_q^{n+1}$ belong to the same equivalence class $[\mathbf{u}]$ if they differ by scalar multiplication, i.e., $\mathbf{u} = \alpha \mathbf{v}$ for some $\alpha \in \mathbb{F}_q$. Consequently, one can view each point $[\mathbf{u}] \in \text{PG}(n, q)$ as a collection of points in \mathbb{F}_q^{n+1} starting from \mathbf{u} and passing through the origin.

The projective space that we will use to construct the decoupling group is $\text{PG}(n, 4)$. The decoupling group is constructed using the check matrix H of the linear code \mathcal{C} . As a reminder, the codeword $\mathbf{c} \in \mathcal{C}$ is the kernel of the check matrix, i.e.

$$H\mathbf{c} = \mathbf{0}. \quad (46)$$

As a first step, we show how to construct a DD group for universal cancellation of all two-body interactions

C_1	C_2	C_3	C_4	C_5
1 0	0 0	1 0	1 0	1 0
0 1	0 0	1 1	0 1	1 1
0 0	1 0	0 1	1 0	1 1
0 0	0 1	1 0	0 1	0 1

C_1	C_2	C_3	C_4	C_5
1	0	1	1	1
ω	0	$1+\omega$	ω	$1+\omega$
0	1	ω	1	$1+\omega$
0	ω	1	ω	ω

C_1	C_2	C_3	C_4	C_5
X	I	X	X	X
Z	I	Y	Z	Y
I	X	Z	X	Y
I	Z	X	Z	Z

(a)

C_1	C_2	C_3	C_4	C_5	C_6	C_7	C_8	C_9	C_{10}	C_{11}	C_{12}	C_{13}	C_{14}	C_{15}
X	Z	Y	I	I	I	X	Z	Y	X	Z	Y	X	Z	Y
Z	Y	X	I	I	I	Y	X	Z	Z	Y	X	Y	X	Z
I	I	I	X	Z	Y	Z	Y	X	X	Z	Y	Y	X	Z
I	I	I	Z	Y	X	X	Z	Y	Z	Y	X	Z	Y	X

(b)

TABLE II: **Universal suppression of two-local and Heisenberg exchange interactions.** These tables illustrate how to derive DD groups from additive projective geometry codes based on a 1-spread in $\text{PG}(3, 2)$. (a) Left: A (complete) 1-spread in $\text{PG}(3, 2)$, where each column represents a line described by two projective points in \mathbb{F}_2^4 . Center: The corresponding projective points in $\text{PG}(3, 4)$ constructed from the 1-spread in $\text{PG}(3, 2)$ using Eq. 53. Right: The generators of a DD group that suppresses universally suppress two-local interactions constructed from projective points in $\text{PG}(3, 4)$. (b) Generators of DD group tailored for spin-qubit systems based on a 1-spread in $\text{PG}(3, 2)$. Each projective point in $\text{PG}(3, 4)$ is expanded into its three equivalent representatives in \mathbb{F}_4^4 , tripling the number of color classes.

from the projective space. We begin by choosing the columns of the check matrix H to correspond to points $[\mathbf{u}]$ in the projective space $\text{PG}(n, 4)$; that is, to equivalence classes of nonzero vectors in \mathbb{F}_4^{n+1} . The total number of such equivalence classes is given by

$$\frac{4^{n+1} - 1}{3}. \quad (47)$$

From the construction of the check matrix, it follows that the code distance is $d \geq 3$. To see this, we proceed by contradiction and assume that there exists a codeword \mathbf{c} with Hamming weight two. This implies the existence of two columns $[\mathbf{u}], [\mathbf{v}]$ that are linearly dependent, i.e.,

$$[\mathbf{u}] = \alpha[\mathbf{v}], \quad (48)$$

for some $\alpha \in \mathbb{F}_4$. However, by definition of projective space, all distinct points $[\mathbf{u}] \in \text{PG}(n, 4)$ are pairwise linearly independent. Thus, no such weight-two codeword can exist, and the minimum distance of the code must be at least three.

Because the check matrix H of the linear code \mathcal{C} is the generator matrix for the dual code \mathcal{C}^\perp , using Theorem IV.1, we can construct an OA from \mathcal{C}^\perp with parameters

$$\text{OA}\left(4^{n+1}, \chi_I = \frac{4^{n+1} - 1}{3}, 4, 2\right). \quad (49)$$

As a result, the decoupling sequence derived from this orthogonal array universally decouples all two-local interaction terms.

We now show how to construct DD sequences that universally decouple all three-local interactions using linear projective geometry code. The key requirement is that the columns of the check matrix H must form a cap set. A cap set (also known as an arc in projective geometry) in $\text{PG}(n, 4)$ is a collection of points $[\mathbf{u}]$ such that no three are collinear. This condition ensures that the corresponding linear code \mathcal{C} has minimum distance $d = 4$, thereby detecting all weight-three errors.

Let n_H denote the number of columns in the check matrix, i.e. the size of the cap set. Then, the orthogonal array constructed from the dual code \mathcal{C}^\perp has parameters

$$\text{OA}(4^{n+1}, \chi_I = n_H, 4, 3). \quad (50)$$

An important remaining question is how to construct a cap set in $\text{PG}(n, 4)$ with the largest possible size. In general, this is a challenging problem in projective geometry. However, explicit constructions of maximal cap sets are known for small values of n [72]. For example, the largest cap set sizes for $n = 2, 3, 4$ are $n_H = 6, 17, 41$ respectively. For higher dimensions n , near-optimal constructions are known, although it is unlikely that physically relevant graphs of solid-state devices will require these large chromatic number χ_I .

2. Additive projective geometry code

In the preceding construction, we employed linear projective geometry codes to design universal DD groups for two-local and three-local interactions. We now show

that if we use additive projective geometry codes [73], we can construct more time-efficient sequences. The key insight is that the field \mathbb{F}_4 , when considered under addition, is isomorphic to $\mathbb{F}_2 \times \mathbb{F}_2$. Exploiting this structure, Ref. [73] demonstrates that the check matrix H of an additive code with parameters $(\chi_I, 2^k, d)_4$ can be constructed from a collection of χ_I lines in the projective space $\text{PG}(2\chi_I - k - 1, 2)$, such that any $d - 1$ lines in the set are linearly independent.

To universally decouple two-local interactions, we require the code \mathcal{C} to have distance $d = 3$. Consequently, we need to choose a collection of χ_I lines in the projective space $\text{PG}(2\chi_I - k - 1, 2)$ such that any 2 lines in the set are linearly independent. This set is known in projective geometry as (partial) 1-spread. The maximum logical dimension k is given by

$$k = 2\chi_I - h \quad (51)$$

where h is the smallest integer number such that $2^h \geq 3\chi_I + 1$ for even h , and $2^h \geq 3\chi_I + 5$ for odd h . As a result, the orthogonal array constructed from \mathcal{C}^\perp has parameter

$$\text{OA}(2^{\min(\lceil \log_2(3\chi_I + 1) \rceil, \lceil \log_2(3\chi_I + 5) \rceil)}, \chi_I, 4, 2). \quad (52)$$

As a simple example, Table II(a) lists a full 1-spread of the projective space $\text{PG}(3, 2)$, where each projective line is represented by two projective points. Each line is further associated with a colored qubit c_i . In Table II(b), we map each projective line in $\text{PG}(3, 2)$ to a projective point in $\text{PG}(3, 4)$ via a simple embedding from $\mathbb{F}_2 \times \mathbb{F}_2$ to \mathbb{F}_4

$$(0, 0) \rightarrow 0, (1, 0) \rightarrow 1, (0, 1) \rightarrow \omega, (1, 1) \rightarrow 1 + \omega. \quad (53)$$

The resulting rows in the table form generators of a DD group capable of suppressing arbitrary two-local interactions.

We note that the above construction uses the same number of colored qubits and time slices in the decoupling sequence as the multi-axis protocol introduced in Ref. [27]. This is not a coincidence. The multi-axis protocol can be understood as implicitly employing an additive code over \mathbb{F}_4 . This connection arises because the Hadamard matrix defines a binary linear code (the Hadamard code), whose rows or columns correspond to codewords. By grouping these rows into Schur sets [74] and mapping from $\mathbb{F}_2 \times \mathbb{F}_2$ to \mathbb{F}_4 , one preserves the additive structure of the binary code. Consequently, our framework naturally includes the protocol from Ref. [27], providing an alternative way to understand its underlying structure.

To universally decouple three-local interactions, we did not find any explicit constructions using additive projective geometry codes in the literature. However, we expect that additive codes could potentially yield slightly more efficient decoupling sequences for three-local interactions as well. We leave the development of such constructions as an interesting direction for future research.

3. Tailored sequences for spin-qubit

We have demonstrated that projective geometry codes enable efficient decoupling of both two-local and three-local interactions, applicable to bang-bang and bounded-control sequences alike. We now present a simplified, tailored construction that universally suppresses single-qubit errors while specifically removing the Heisenberg exchange and scalar chirality interactions, the naturally occurring residual many-body interactions in spin-qubit platforms.

Let us first focus on the two-body Heisenberg exchange interactions. The main idea is to modify the columns of the check matrix such that no codeword corresponds to a term in the Heisenberg exchange interaction. Specifically, no weight-two codeword of the form $[1, 1], [\omega, \omega], [1 + \omega, 1 + \omega]$ is allowed. In the linear projective geometry code construction, only one representative for each projective equivalence class $[\mathbf{u}]$ is used as a column in the check matrix. As an example, the three equivalent representations of $[(1, \omega)]$ are

$$[(1, \omega)] = \{(1, \omega), (\omega, 1 + \omega), (1 + \omega, 1)\} \quad (54)$$

The key observation is that if we include all projective points in the equivalence class $[\mathbf{u}]$ as separate columns of the check matrix H , no Heisenberg exchange terms arise as codewords. This effectively increases the number of allowed colors χ_I in the decoupling sequence by three times.

A similar strategy also applies to additive projective geometry codes: for each line in the projective space, there exist three distinct representations that also avoid Heisenberg exchange terms as codewords. As an illustration, Table II(c) presents a tailored DD group designed to detect Heisenberg exchange interactions, derived from the construction in Table II(b). Notably, this construction increases the number of color classes from 5 to 15 while retaining the same number of generators. In the case of the multi-axis protocol introduced in Ref. [27], this modification is equivalent to cyclically permuting the rows in the Schur set.

When applying this straightforward extension to Fig. 6(b), under the assumption of residual Heisenberg exchange interactions, the tailored decoupling sequence still requires four generators, matching the number needed for a universal sequence that suppresses all two-local interactions. Therefore, for $\chi_I = 4, 5$ this basic approach does not yield a shorter sequence. However, in Appendix C, we present optimized tailored sequences for these specific cases that require only three generators, offering a reduction in sequence length.

Through exhaustive numerical search, we confirm that this extended construction yields a near-optimal number of color classes for decoupling at fixed sequence lengths $L = 16, 32$, and 64 . However, we note that shorter sequences, such as those of length $L = 4$ (i.e. Eq. (30)) and $L = 8$ are also possible, albeit supporting fewer

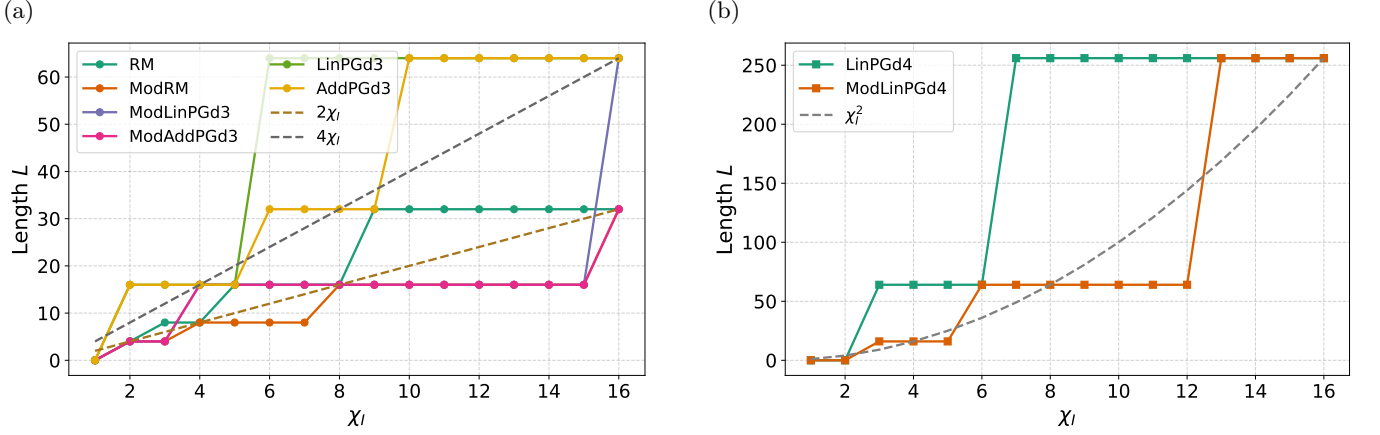


FIG. 7: **Scaling of decoupling sequences.** Scaling of sequence length L with the chromatic number χ_I for the code constructions listed in Table III. (a) For comparison, the linear baseline $L = 4\chi_I$ is shown in black. All codes with distance $d = 3$ exhibit linear scaling in χ_I , while those with $d = 4$ show quadratic scaling, consistent with the scaling reported in Ref. [30].

Scheme	# Gen.	2-local	3-local	Bounded
Mod. RM	$\lceil \log_2(\chi_I + 1) \rceil$	ZZ	–	Yes
RM	$\lceil \log_2(\chi_I) \rceil + 1$	ZZ	ZZZ	Yes
Lin-PG ($d = 3$)	$2 \log_4(3\chi_I + 1)$	All	–	Yes
Lin-PG ($d = 4$)	6, 8, 10*	All	All	Yes
Add-PG ($d = 3$)	$\log_2(3\chi_I + 1) \setminus \log_2(3\chi_I + 5)$	All	–	Yes
Mod. Lin-PG ($d = 3$)	$2 \log_4(\chi_I + 1)$	Hexch.	–	No
Mod. Lin-PG ($d = 4$)	4, 6, 8, 10**	Hexch.	Chir.	No
Mod. Add-PG ($d = 3$)	$\log_2(\chi_I + 1) \setminus \log_2(\chi_I + 5)$	Hexch.	–	No

TABLE III: **Comparison of decoupling sequences.** “# Gen.” indicates the number of additive code generators. “Hexch.” = Heisenberg exchange; “Chir.” = scalar chirality; “All” = universal decoupling. Asterisked values * and ** denote number of additive generators for $\chi_I = 6, 17, 41$ and $\chi_I = 5, 12, 34, 82$ respectively. “Bounded” indicates whether the scheme is compatible with bounded control (all work with bang-bang control).

color classes. Such compact sequences can be systematically constructed by iteratively removing one generator from DD group with longer sequence length L at a time and reducing the number of color classes, while ensuring that the resulting DD group still suppresses arbitrary single-qubit errors and detects Heisenberg exchange interactions.

When including the three-body scalar chirality interaction, a similar strategy can be applied to increase the number of allowed colors in the decoupling sequence. However, the additional constraints imposed by this interaction limit the modification of the projective geometry code’s columns to only doubling the color count χ_I .

Let us apply this idea to the quotient graph in Fig. 6(b). We begin by constructing a cap set in $\text{PG}(2, 4)$, which corresponds to a universal DD sequence that decouples all three-local interactions among six qubits. This cap set is given by the additive generators of the

self-dual hexacode [75]

$$\begin{pmatrix} 1 & 0 & 0 & 1 & 1 & \omega \\ 0 & 1 & 0 & 1 & \omega & 1 \\ 0 & 0 & 1 & \omega & 1 & 1 \\ \omega & 0 & 0 & \omega & \omega & 1 + \omega \\ 0 & \omega & 0 & \omega & 1 + \omega & \omega \\ 0 & 0 & \omega & 1 + \omega & \omega & \omega \end{pmatrix}. \quad (55)$$

To construct a tailored sequence, we remove the first three columns and focus on the remaining three. We then apply the expansion strategy by selecting one of these columns (e.g. the last) and multiplying it by ω to generate a new fourth column

$$\begin{pmatrix} 1 & 1 & \omega & 1 + \omega \\ 1 & \omega & 1 & \omega \\ \omega & 1 & 1 & \omega \\ \omega & \omega & 1 + \omega & 1 \\ \omega & 1 + \omega & \omega & 1 + \omega \\ 1 + \omega & \omega & \omega & 1 + \omega \end{pmatrix} \rightarrow \begin{pmatrix} X & X & Z & Y \\ X & Z & X & Z \\ Z & X & X & Z \\ Z & Z & Y & X \\ Z & Y & Z & Y \\ Y & Z & Z & Y \end{pmatrix}. \quad (56)$$

The resulting DD sequence suppresses both the Heisenberg exchange interactions and the scalar chirality terms. However, it stills contains six generators. By mapping the generator set to a minimum covering problem, as described in Sec. IV D, we find that only four of these generators are necessary to detect all relevant interaction term

$$\begin{pmatrix} X & X & Z & Y \\ X & Z & X & Z \\ Z & Z & Y & X \\ Z & Y & Z & Y \end{pmatrix}. \quad (57)$$

Without going into detail, we also report that applying the same expansion strategy to one of the unused original columns (e.g., the first column) allows us to increase the number of interaction colors to $\chi_I = 5$ while still requiring only four generators

$$\begin{pmatrix} Z & X & X & Z & Y \\ Y & Z & X & X & Z \\ Y & Z & Z & Y & X \\ X & Y & Z & Z & Y \end{pmatrix}. \quad (58)$$

These optimized sequences achieves the same suppression with only $L = 16$ pulses, compared to a universal DD sequence of length $L = 64$, yielding a fourfold reduction in sequence length.

We emphasize that the expansion approach is effective primarily for bang-bang sequences. Under bounded control, finite pulse durations can lead to Heisenberg exchange or scalar chirality interactions transforming into other three-local terms that the sequence may not cancel. In such cases, alternative constructions may be required to obtain tailored, time-efficient bounded-control DD sequences. Alternatively, one may resort to the universal DD sequences discussed in Sec. VB 1, which, although potentially longer, suppress all three-local interactions. Finally, we note that shorter sequences can often be obtained by systematically removing generators from a universal sequence, one at a time, as demonstrated above. This process might reduces the number of supported color classes but preserving the required decoupling properties. Developing such compact, tailored sequences remains an interesting direction for future work.

For completeness, we summarize the parameters of all our constructions in Table III, along with their applicability to either bang-bang sequences or bounded-control sequences. Since all the sequences we consider permit universal DD, we only specify which types of two-local and three-local interactions are eliminated by each construction.

We also analyze the sequence lengths as a function of the chromatic number χ_I . To visualize this, in Fig. 7a we show the scaling of different DD sequences that suppress two-local interactions as the chromatic number χ_I increases; in Fig. 7b, we focus on sequences targeting three-local interactions. In both cases, we compare the scaling behavior of the sequence lengths against ideal linear and quadratic scaling.

For two-local interactions, we find that the universal constructions scale linearly with sequence length $4\chi_I$, while the tailored constructions scale more compactly with $2\chi_I$. In the case of three-local interactions, both universal and tailored constructions exhibit quadratic scaling $L \propto \chi_I^2$, but the tailored sequences have a smaller prefactor, leading to more efficient implementations. These scaling behaviors are consistent with those of Ref. [30].

C. Digital-analog simulation

In the previous section, we showed how to construct DD sequences that suppress residual interactions within the system and its environment. In this section, we demonstrate how such sequences can also be leveraged for Hamiltonian simulation and digital-analog quantum computing. For concreteness, we consider the Kitaev's honeycomb lattice toy model, described by the Hamiltonian [76]

$$H_{\text{comb}} = -\frac{J_x}{4} \sum_{\langle ij \rangle_r} X_i X_j - \frac{J_y}{4} \sum_{\langle ij \rangle_g} Y_i Y_j - \frac{J_z}{4} \sum_{\langle ij \rangle_b} Z_i Z_j, \quad (59)$$

where the sum is taken over the red (r), blue (b), and green (g) colored edges in Fig. 8a. This model is exactly solvable by using a mapping to Majorana fermions and exhibits both gapped and gapless phases depending on whether the coupling strengths J_x, J_y, J_z satisfy the triangle inequality [76]. Here, we focus on simulating the system deep in the gapless phase, where $J_x = J_y = J_z = J$.

We assume that the native analog Hamiltonian of the spin qubit device comprises Heisenberg interactions

$$H_{\text{analog}} = \sum_{\langle ij \rangle} \frac{J}{4} (X_i X_j + Y_i Y_j + Z_i Z_j). \quad (60)$$

We aim to simulate the target Hamiltonian H_{comb} using H_{analog} . First, because the native interactions are isotropic, with XX , YY , and ZZ couplings have the same amplitude, we must design a DD group that selectively preserves only one type of interaction (either XX , YY , or ZZ) based on the edge label in the honeycomb lattice. Second, once the desired interaction type is isolated, we must flip the global sign of the Hamiltonian to convert the native antiferromagnetic coupling (positive J) into a ferromagnetic one (negative J).

As in previous sections, we begin by identifying the effective number of qubits in Kitaev's honeycomb model. If we were to universally decouple all interactions, the honeycomb lattice would be trivially 2-colorable. However, because we aim to selectively preserve certain interactions, the effective model becomes more complex.

In particular, due to the link-dependent interaction terms in the Hamiltonian, the symmetry of the model reduces the problem to an effective system involving six

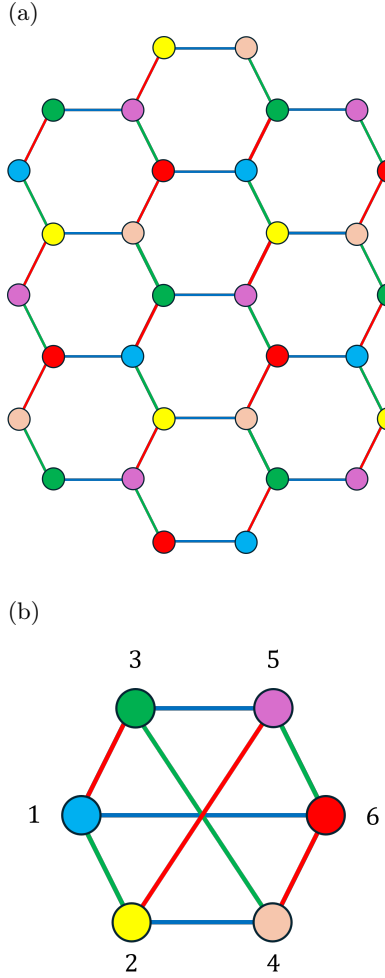


FIG. 8: **Dynamical quantum simulation of the Kitaev model.** (a) A finite-size Kitaev honeycomb lattice, where edges are colored red, blue, and green to represent $X_i X_j$, $Y_i Y_j$, and $Z_i Z_j$ interactions, respectively. The labels 1 through 6 indicate the equivalence classes of qubits under the vertex color partition which respects the edges coloring, not individual physical qubits. (b) The folded Kitaev lattice (i.e., the quotient graph) obtained by collapsing all qubits within the same equivalence class. Compared to the standard unit cell, the quotient graph includes three additional edges (2-5), (3-4), and (1-6) that arise from the folding.

qubits. In Fig. 8a, we color the qubits that are equivalent under the translation symmetry of the honeycomb lattice. The resulting quotient graph, formed by identifying these symmetry-equivalent sites, contains six effective colored qubits. There are three extra edges appear between opposite effective vertices, as shown in Fig. 8b.

To demonstrate the power of the effective graph in Fig. 8b, we use the simple algorithm presented in Section IV D to find the minimal DD group for the bang-bang sequence. We also explicitly construct a DD group

for the bounded sequence, see Appendix D. Using the same terminology as before, we associate $H_S^{\parallel} = H_{\text{comb}}$. Consequently, the remaining interactions belong to the list H_S^{\perp} .

By finding the kernel of the linear map defined in Eq. (36), we identify four operators spanning the kernel space that commute with H_S^{\parallel} . These operators are

$$W_1 = Z_1 X_2 Z_3 X_4, \quad W_2 = X_3 Z_4 X_5 Z_6, \quad (61a)$$

$$W_3 = X_1 Z_2 Z_5 X_6, \quad W_4 = Y_2 X_3 X_5 Y_6, \quad (61b)$$

and are closely related to a known symmetry of the Kitaev honeycomb model, namely the plaquette operator [76]

$$W_p = Z_1 X_2 Y_3 Y_4 X_5 Z_6. \quad (62)$$

One can verify that $W_1 W_2 = W_p$ and $W_3 W_4 = W_p$, that is, each pair provides a decomposition of the original plaquette symmetry. The emergence of these subsymmetries is expected: since the effective Kitaev honeycomb model arises from folding the original lattice, it can exhibit additional symmetries not present in the unfolded geometry.

If we take W_p as a generator of a DD group \mathcal{G} , the resulting sequence effectively removes the interaction terms along the outer edges of the hexagon in Fig. 8b, aligning the system's dynamics with that of the Kitaev model. However, the inner-edge interactions commute with W_p , so they are not eliminated by this sequence and remain in the effective Hamiltonian. This again reflects the presence of the subsymmetries introduced by lattice folding.

Either by numerically solving the associated minimum-covering problem or by manually verifying it, we find that using either the pair (W_1, W_2) or (W_3, W_4) as generators is sufficient to construct a DD group \mathcal{G} for the bang-bang sequence. Consequently, the effective Hamiltonian have the same interaction as shown in the edges of Fig. 8b. However, the global site is opposite of what it should be, i.e $H_S^{\parallel} = -H_{\text{comb}}$.

To flip the global sign of the Hamiltonian, we use the following three operators

$$X_1 X_4 X_5, \quad Y_1 Y_4 Y_5, \quad Z_1 Z_4 Z_5. \quad (63)$$

Each of these operators commutes only with edges involving the same type of Pauli interaction and anti-commutes with the rest. For instance, $X_1 X_4 X_5$ commute with $X_1 X_3$ but anti-commutes with $Z_1 Z_2$. Consequently, by sequentially conjugating the effective Hamiltonian H_S^{\parallel} with these operators, we flip the sign of H_S^{\parallel} , yielding the target Kitaev Hamiltonian:

$$\sum_{P \in \{X, Y, Z\}} P_1 P_4 P_5 H_S^{\parallel} P_1 P_4 P_5 = H_{\text{comb}}. \quad (64)$$

Alternatively, we can view the three operators in Eq. (63) as (almost) forming a group. By including the identity operator, they generate the group

$$\langle X_1 X_4 X_5, Z_1 Z_4 Z_5 \rangle. \quad (65)$$

Twirling over the full group (including the identity) would suppress H_S^{\parallel} entirely. However, omitting the identity from the twirling set leads to the desired sign-flipping behavior described above. In conclusion, a full DD cycle implementing this sign-flipping mechanism consists of three such conjugations, each comprising a 4-element DD sequence, resulting in a total sequence length of $L = 3 \times 4 = 12$.

In this section, we have demonstrated how to construct a bang-bang sequence that simulates Kitaev's honeycomb model using only Heisenberg exchange interactions. In Appendix D, we extend this construction to bounded-control sequences for the same task. While the bounded-control sequence is significantly longer, it offers the advantage of allowing independent tuning of the interaction strengths J_x, J_y and J_z through the appropriate choice of control pulses.

VI. CONCLUSION AND OUTLOOK

We introduced a general unified framework for constructing time-efficient DD sequences on quantum devices with arbitrary connectivity. First, we showed how the problem of designing DD sequences for k -local interactions can be significantly simplified by leveraging symmetries arising from the hypergraph coloring of the interaction graph. This reduction leads to a simplified problem whose size depends only on the chromatic number of the interaction graph, which in turn is determined by the topology of the device, rather than its total number of qubits. Second, we established a conceptual bridge between DD sequences and classical additive codes. In particular, when the decoupling group is a subgroup of the single-qubit Pauli group, DD sequences can be interpreted as quaternary error-detecting codes over \mathbb{F}_4 , providing a unified algebraic framework to analyze and design DD protocols. Third, we constructed explicit, time-efficient DD sequences tailored to both superconducting qubits and spin qubits that are capable of selectively suppressing arbitrary interactions that are up to three-local. An additional notable advantage of our method is that many of the sequences are compatible with bounded-control implementations, relaxing the conventional assumption of instantaneous pulses and making them more suitable for near-term quantum hardware.

Beyond error suppression, we also demonstrated that the code-theoretic perspective on DD provides an effective way to engineer effective Hamiltonians useful for digital-analog quantum simulations. To be concrete, we showed a practical example of how our framework can be applied to simulate Kitaev's honeycomb model on spin-qubit platforms, highlighting the versatility of the approach. Building on the results of Refs. [24, 77], our framework can further be applied to isolate and measure specific interactions within the system. Our results contribute to scalable near-term quantum computation and simulation by providing practically implementable

sequences that protect against coherent errors from residual interactions and environmental noise.

Several interesting directions remain open for future investigation. Our current constructions are based on DD groups that are subgroups of the Pauli group, which naturally support a mapping to additive codes over \mathbb{F}_4 . An important next step is to extend this framework to DD groups that are subgroups of the Clifford group [78, 79]. Such sequences could achieve symmetrization of the system dynamics [41, 78], and could become an additional tool for Hamiltonian simulation [29]. In fact, Ref. [79] is closely aligned in spirit with our work, leveraging the symmetries of specific spin–spin interactions to design efficient decoupling sequences based on single-qubit Clifford groups. Another promising direction is to explore the robustness of our DD sequences. While our methods assume idealized pulses, known DD sequences exist that are robust against pulse imperfections [11, 12, 80, 81]. Developing a systematic procedure to generalize our DD framework to make it more robust is a stimulating question. Finally, it remains an open challenge to integrate the hypergraph-coloring approach with the Uhrig sequence family [15–17], which is known to provide arbitrary-order noise suppression. However, the sequence length might increase significantly with increasing system size.

VII. ACKNOWLEDGMENT

We thank members of the Bosco, Rimbach-Russ, Terhal, and Vandersypen groups for valuable discussions. We are grateful to Pablo Cova Fariña for pointing out that the Kitaev honeycomb model can be simulated using a dynamical decoupling sequence of length $L = 4$. This research was supported by the EU through the H2024 QLSI2 project, by the Army Research Office under Award Number: W911NF-23-1-0110, and by NCCR Spin (grant number 225153). The views and conclusions contained in this document are those of the authors and should not be interpreted as representing the official policies, either expressed or implied, of the Army Research Office or the U.S. Government. The U.S. Government is authorized to reproduce and distribute reprints for Government purposes notwithstanding any copyright notation herein.

Appendix A: Bounded control sequence

In this appendix, we review the bounded-control scheme for dynamical decoupling sequences [31]. The key idea is that the control operations are generated by a set of generators of the decoupling group \mathcal{G} . The decoupling sequence is implemented by continuously and smoothly evolving between elements of \mathcal{G} via these generators, rather than through instantaneous (bang-bang) pulses.

Let $\Gamma_{\mathcal{G}} = \{\gamma_1, \dots, \gamma_m\}$ denote a generating set of the decoupling group \mathcal{G} . We assume that each generator $\gamma_j \in \Gamma_{\mathcal{G}}$ can be implemented over a uniform time interval Δ using a time-dependent control Hamiltonian $h_{\gamma_j}(t)$ such that

$$\gamma_j = \mathcal{T} \exp \left(-i \int_0^\Delta dt h_{\gamma_j}(t) \right). \quad (\text{A1})$$

We define $\text{Cay}(\mathcal{G}, \Gamma_{\mathcal{G}})$ as the Cayley graph of the group \mathcal{G} with respect to the generating set $\Gamma_{\mathcal{G}}$ [30, 31]. The Cayley graph $\text{Cay}(\mathcal{G}, \Gamma_{\mathcal{G}})$ is a directed graph where each vertex corresponds to a group element $g_i \in \mathcal{G}$. There is a directed edge from vertex g_i to vertex g_{i+1} , labeled by the generator γ_k iff $g_{i+1} = \gamma_k g_i$.

In the bounded control scheme, the control propagator U_c follows a balanced cycle in $\text{Cay}(\mathcal{G}, \Gamma_{\mathcal{G}})$. A balanced cycle is defined as a closed path that traverses each edge labeled by generator γ_j exactly λ_j times, where λ_j is a positive integer. Since $\text{Cay}(\mathcal{G}, \Gamma_{\mathcal{G}})$ is a regular graph, such a cycle always exists, and its length is exactly $|L| = |\mathcal{G}|(\sum_j \lambda_j)$. For clarity, we denote $\Lambda = \sum_j \lambda_j$.

The control propagator U_c starts at the identity element of the group \mathcal{G} and evolves according to a path $L = \{l_1, \dots, l_{|L|}\}$, where each $l_i \in \Gamma_{\mathcal{G}}$ specifies a generator. Due to the deterministic structure of the Cayley graph, each vertex admits a unique outgoing edge for a given generator, ensuring an unambiguous evolution along the path. The control propagator is defined piecewise over intervals of duration Δ as

$$U_c[(j-1)\Delta + \tau] = u_{l_j}(\tau)U_c[(j-1)\Delta], \quad (\text{A2})$$

where

$$u_{l_j}(\tau) = \mathcal{T} \exp \left(-i \int_0^\tau dt h_{l_j}(t) \right) \quad (\text{A3})$$

for $\tau \in [0, \Delta]$.

Using Eq. (6), the average Hamiltonian \overline{H} can be grouped into elements of the generating set $\Gamma_{\mathcal{G}}$, namely

$$\overline{H} = \Pi_{\mathcal{G}}(F_{\Gamma}(H)) \quad (\text{A4a})$$

where the channel $F_{\Gamma}(H)$ is defined as

$$F_{\Gamma}(H) = \left(\sum_{\gamma_j \in \Gamma} \frac{\lambda_j}{\Lambda \Delta} \int_0^\Delta dt u_{\gamma_j}^\dagger(t) H u_{\gamma_j}(t) \right). \quad (\text{A5})$$

As a result, the total length of the bounded-control sequence increases by an additional factor proportional to the number of generators in $\Gamma_{\mathcal{G}}$.

Since F_{Γ} is a trace-preserving quantum channel, it maps traceless Hamiltonians to traceless operators. Therefore, if U_g defines an irreducible representation of \mathcal{G} , the decoupling sequence $\Pi_{\mathcal{G}}$ also decouples $F_{\Gamma}(H)$. However, in the more general case where U_g is not irreducible, the decoupling is guaranteed only if $F_{\Gamma}(H)$ does

not acquire components within the invariant subspace of $\Pi_{\mathcal{G}}$. Therefore, successful decoupling under bounded control requires designing both the decoupling group \mathcal{G} and its generator set $\Gamma_{\mathcal{G}}$ such that neither H nor $F_{\Gamma}(H)$ has support in the invariant subspace preserved by the bang-bang decoupling $\Pi_{\mathcal{G}}$.

Appendix B: Superconducting qubit (bounded control)

In the main text, we showed how to construct a bang-bang decoupling sequence tailored to superconducting qubits using the binary Reed-Muller code. In this appendix, we extend that construction to the bounded-control setting, demonstrating how the same code framework can be adapted when only finite-time control pulses are available.

As a first step, we describe how to implement the control pulses associated with the generators of the decoupling group in the quotient graph $I'_{\text{Dev}}/C[I_{\text{Dev}}]$. Each generator $\gamma_i \in \mathcal{G}$ is a Pauli string of the form

$$\gamma_{p_i} = [\gamma_{p_i}]_1 \otimes \dots \otimes [\gamma_{p_i}]_{\chi_G}, \quad (\text{B1})$$

where each element $[\gamma_{p_i}]_k$ acts on the k -th color class. To lift this operator from the quotient graph back to the original graph, we impose that $[\gamma_{p_i}]_k$ acts uniformly on all qubits belonging to the color class c_k . That is, for each qubit $q_j \in c_k$, the same single-qubit Pauli operator $[\gamma_{p_i}]_k$ is applied.

We assume the control Hamiltonian used to implement γ_{p_i} is composed of local, single-qubit Pauli operators, and is given by

$$h_{\gamma_{p_i}}(t) = \sum_{c_k \in C[G_{\text{Dev}}]} \sum_{q_j \in c_k} A_k^{q_j}(t) [\gamma_{p_i}]_k^{(q_j)}, \quad (\text{B2})$$

where $[\gamma_{p_i}]_k^{(q_j)}$ denotes the local Pauli operator assigned to qubit $q_j \in c_k$ and $A_k^{q_j}(t)$ are the time-independent amplitude of the pulses. The pulse amplitudes are controlled such that

$$\gamma_{p_i} = \mathcal{T} \exp \left(-i \int_0^\Delta h_{\gamma_{p_i}}(t) \right). \quad (\text{B3})$$

The decomposition ensures that each control pulse can be executed using local, parallel single-qubit operations in a way that respects the color partition of the interaction graph.

As an example, we show that, under the substitution $0 \rightarrow I$ and $1 \rightarrow X$, the bounded-control decoupling sequence constructed from the $RM(1, m)$ code continues to suppress all Z -type Pauli strings of weight up to three. Since the generators are all X -type Pauli strings, the control Hamiltonian implements rotations around the X -axis. As a result, due to the finite duration of the control pulses, the channel F_{Γ} rotates a Pauli Z operator into linear combination of Z and Y

$$Z \rightarrow \cos(\alpha)Z + \sin(\alpha)Y. \quad (\text{B4})$$

The key insight is that the Y Pauli operator remains detectable by the X -type generators, since X anticommutes with Y . Therefore, any nontrivial operator in the image of F_Γ still anticommutes with some generator in the decoupling group \mathcal{G} . As a result, \mathcal{G} not only eliminates all Z -type strings of weight three or less but also cancels their rotated counterparts generated by the bounded-control channel F_Γ thereby ensuring effective suppression even under bounded-control sequence.

For the universal bounded-control sequence constructed from the RM(1, m) code, we cannot simply apply the substitution 0 with I or Z and 1 with X and Y as done in the main text. This is because, under these substitutions, the channel F_Γ generally maps any Z -type Pauli string into a linear combination of arbitrary Pauli strings of the same weight, involving any mixture of X , Y and Z . Consequently, some of these terms may commute with all generators of the decoupling group \mathcal{G} and therefore are not suppressed by the sequence. This highlights a key limitation of bounded-control schemes for universal decoupling: unless the decoupling group is carefully designed, the sequence may fail to eliminate all error terms.

To overcome this issue, we introduce an additional generator of the form

$$Z_{c_1} \otimes Z_{c_2} \otimes \cdots \otimes Z_{c_{\chi_I}}, \quad (\text{B5})$$

which applies a global Z operator to each color class. This operator commutes with all Z -type Pauli strings, meaning the corresponding control Hamiltonian does not introduce any unwanted interactions that would require further cancellation. Crucially, it anticommutes with any single-qubit X or Y operator acting on a colored qubit, thereby enabling universal decoupling of single-qubit errors. As a result, the total length of the bounded-control decoupling sequence becomes

$$2^{\lceil \log_2(\chi_I + 1) \rceil + 1} (\lceil \log_2(\chi_I + 1) \rceil + 1) \sim O(\chi_I \log \chi_I), \quad (\text{B6})$$

which scales linearly with the chromatic number χ_I , with only a logarithmic overhead arising from the bounded-control implementation.

Appendix C: Tailored sequence for two-local interactions in spin-qubit architecture with $\chi_I = 4, 5$

In this appendix, we discuss how to construct tailored sequence for two-local interactions in spin-qubit architecture with $\chi_I = 4, 5$ using only three generators. The construction is based on additive code in $\text{PG}(2, 2)$.

We begin by labeling the seven points in the projective

plane $\text{PG}(2, 2)$ as follows

$$\begin{bmatrix} P_1 & (1, 0, 0)^T \\ P_2 & (0, 1, 0)^T \\ P_3 & (0, 0, 1)^T \\ P_4 & (1, 1, 0)^T \\ P_5 & (1, 0, 1)^T \\ P_6 & (0, 1, 1)^T \\ P_7 & (1, 1, 1)^T \end{bmatrix}. \quad (\text{C1})$$

Throughout this section, we represent a line in $\text{PG}(2, 2)$ by an ordered pair of points (P_i, P_j) . The requirement that the code detects the Heisenberg exchange interaction translates into the following constraints on pairs of lines (P_i, P_j) and (P_n, P_m)

$$P_i \neq P_n, P_j \neq P_m, \quad (\text{C2a})$$

$$P_i + P_j \neq P_n + P_m. \quad (\text{C2b})$$

These constraints can be reformulated as a combinatorial problem reminiscent of a Sudoku puzzle. Consider a 7×7 table whose rows and columns are labeled by the points P_1 through P_7 . Each entry in the table is defined as the sum of the corresponding row and column labels

$$\begin{array}{c|ccccccc} & P_1 & P_2 & P_3 & P_4 & P_5 & P_6 & P_7 \\ \hline P_1 & & P_4 & P_5 & P_2 & P_3 & P_7 & P_6 \\ P_2 & P_4 & & P_6 & P_1 & P_7 & P_3 & P_5 \\ P_3 & P_5 & P_6 & & P_7 & P_1 & P_2 & P_4 \\ P_4 & P_2 & P_1 & P_7 & & P_6 & P_5 & P_3 \\ P_5 & P_3 & P_7 & P_1 & P_6 & & P_4 & P_2 \\ P_6 & P_7 & P_3 & P_2 & P_5 & P_4 & & P_1 \\ P_7 & P_6 & P_2 & P_4 & P_3 & P_5 & P_1 & \end{array} \quad (\text{C3})$$

The problem then becomes finding the largest possible subset of table entries such that no row, column, or resulting entry value appears more than once. This ensures that the pairwise constraints on lines are satisfied. For small instances such as this 7×7 table, heuristic search algorithms can be used to efficiently find such maximal subsets.

One such solution is the following set of line triples

$$\{(P_1, P_2, P_4), (P_2, P_3, P_6), (P_3, P_4, P_7)\} \quad (\text{C4a})$$

$$\{(P_4, P_6, P_5), (P_5, P_7, P_2)\}. \quad (\text{C4b})$$

Converting these lines back into their point coordinates in $\text{PG}(2, 2)$ and then into Pauli operators, we obtain the following set of additive generators for the tailored decoupling group:

$$\begin{array}{c|ccccc} \hline & C_1 & C_2 & C_3 & C_4 & C_5 \\ \hline \begin{bmatrix} 1 & 0 & 0 & 0 & 1 & 1 & 0 & 1 & 1 \end{bmatrix} & \rightarrow & \begin{bmatrix} C_1 & C_2 & C_3 & C_4 & C_5 \\ X & I & Z & X & Y \\ Z & X & Z & Y & Z \\ I & Z & X & Z & Y \end{bmatrix} \\ \begin{bmatrix} 0 & 1 & 1 & 0 & 0 & 1 & 1 & 0 & 1 \end{bmatrix} & \rightarrow & \begin{bmatrix} C_1 & C_2 & C_3 & C_4 & C_5 \\ X & I & Z & X & Y \\ Z & X & Z & Y & Z \\ I & Z & X & Z & Y \end{bmatrix} \\ \begin{bmatrix} 0 & 0 & 0 & 1 & 1 & 0 & 0 & 1 & 1 \end{bmatrix} & \rightarrow & \begin{bmatrix} C_1 & C_2 & C_3 & C_4 & C_5 \\ X & I & Z & X & Y \\ Z & X & Z & Y & Z \\ I & Z & X & Z & Y \end{bmatrix} \end{array} \quad (\text{C5})$$

It is straightforward to verify that this decoupling group universally suppresses all single-qubit terms as well as

Heisenberg exchange interactions in systems with $\chi_I = 4$ or 5.

In general, finding the largest set of ordered point pairs in $\text{PG}(n, 2)$ that satisfy the constraints of Eqs. C2 is computationally difficult. In fact, this problem can be shown to be NP-hard, as it is a specific instance of the well-known 3-dimensional matching problem. Consequently, the simple expansion strategy presented in the main text should be viewed as a heuristic algorithm. While effective for small instances, it leaves significant room for optimization in larger settings.

Appendix D: Simulating Kitaev's honeycomb model with bounded control

For the bounded-control setting, however, additional terms can be generated through the channel F_Γ . Accounting for these terms, we numerically find that all four operators W_1, W_2, W_3 , and W_4 are required to fully decouple the undesired interactions. The resulting sequence removes all two-local terms except those in H_{comb} . Moreover, by tuning the control Hamiltonian appropriately, it becomes possible to simulate an anisotropic Kitaev model with $J_x \neq J_y \neq J_z$, even if the native system Hamiltonian consists solely of Heisenberg exchange interactions. The total number of time slices in the bounded-control protocol is then given by

$$2^4 \times 4 = 64. \quad (\text{D1})$$

[1] E. L. Hahn, *Phys. Rev.* **80**, 580 (1950).

[2] S. Meiboom and D. Gill, *Review of Scientific Instruments* **29**, 688 (1958).

[3] A. Maudsley, *Journal of Magnetic Resonance* (1969) **69**, 488 (1986).

[4] A. Brinkmann, *Concepts in Magnetic Resonance Part A* **45**, e21414 (2016).

[5] A. Brinkmann, *Journal of Magnetic Resonance Open* **23**, 100191 (2025).

[6] D. Vitali and P. Tombesi, *Phys. Rev. A* **59**, 4178 (1999).

[7] L. Viola and S. Lloyd, *Phys. Rev. A* **58**, 2733 (1998).

[8] L. Viola, E. Knill, and S. Lloyd, *Physical Review Letters* **82**, 2417 (1999).

[9] L.-M. Duan and G.-C. Guo, *Physics Letters A* **261**, 139 (1999).

[10] T. Gullion, D. B. Baker, and M. S. Conradi, *Journal of Magnetic Resonance* (1969) **89**, 479 (1990).

[11] Z.-H. Wang, W. Zhang, A. M. Tyryshkin, S. A. Lyon, J. W. Ager, E. E. Haller, and V. V. Dobrovitski, *Phys. Rev. B* **85**, 085206 (2012).

[12] Z.-H. Wang, G. de Lange, D. Ristè, R. Hanson, and V. V. Dobrovitski, *Phys. Rev. B* **85**, 155204 (2012).

[13] J. R. West, B. H. Fong, and D. A. Lidar, *Phys. Rev. Lett.* **104**, 130501 (2010).

[14] S. Pasini and G. S. Uhrig, *Journal of Physics A: Mathematical and Theoretical* **43**, 132001 (2010).

[15] G. S. Uhrig, *Phys. Rev. Lett.* **98**, 100504 (2007).

[16] Z.-Y. Wang and R.-B. Liu, *Physical Review A—Atomic, Molecular, and Optical Physics* **83**, 022306 (2011).

[17] W. Yang and R.-B. Liu, *Physical review letters* **101**, 180403 (2008).

[18] P. Szałkowski, G. Ramon, J. Krzywda, D. Kwiatkowski, *et al.*, *Journal of Physics: Condensed Matter* **29**, 333001 (2017).

[19] G. A. Álvarez and D. Suter, *Phys. Rev. Lett.* **107**, 230501 (2011).

[20] G. A. Paz-Silva and D. A. Lidar, *Scientific reports* **3**, 1530 (2013).

[21] A. Vezvaei, V. Tripathi, M. Morford-Oberst, F. Butt, V. Kasatkin, and D. A. Lidar, *Demonstration of high-fidelity entangled logical qubits using transmons* (2025), arXiv:2503.14472 [quant-ph].

[22] V. Tripathi, H. Chen, M. Khezri, K.-W. Yip, E. Levenson-Falk, and D. A. Lidar, *Phys. Rev. Appl.* **18**, 024068 (2022).

[23] J. Qiu, Y. Zhou, C.-K. Hu, J. Yuan, L. Zhang, J. Chu, W. Huang, W. Liu, K. Luo, Z. Ni, *et al.*, *Physical Review Applied* **16**, 054047 (2021).

[24] B. Evert, Z. G. Izquierdo, J. Sud, H.-Y. Hu, S. Grabbe, E. G. Rieffel, M. J. Reagor, and Z. Wang, arXiv preprint arXiv:2403.07836 (2024).

[25] J. S. Waugh, L. M. Huber, and U. Haeberlen, *Phys. Rev. Lett.* **20**, 180 (1968).

[26] K. Agarwal and I. Martin, *Physical Review Letters* **125**, 080602 (2020).

[27] A. F. Brown and D. A. Lidar, arXiv preprint arXiv:2406.13901 (2024).

[28] P. Coote, R. Dimov, S. Maity, G. S. Hartnett, M. J. Biercuk, and Y. Baum, *PRX Quantum* **6**, 010332 (2025).

[29] J. Choi, H. Zhou, H. S. Knowles, R. Landig, S. Choi, and M. D. Lukin, *Phys. Rev. X* **10**, 031002 (2020).

[30] A. D. Bookatz, M. Roetteler, and P. Wocjan, *IEEE Transactions on Information Theory* **62**, 2881–2894 (2016).

[31] L. Viola and E. Knill, *Phys. Rev. Lett.* **90**, 037901 (2003).

[32] M. Rötteler and P. Wocjan, *IEEE Transactions on Information Theory* **52**, 4171–4181 (2006).

[33] C. Tong, H. Zhang, and B. Pokharel, arXiv preprint arXiv:2403.02294 (2024).

[34] A. Rahman, D. J. Egger, and C. Arenz, *Physical Review Applied* **22**, 054074 (2024).

[35] F. Casas, *Journal of Physics A: Mathematical and Theoretical* **40**, 15001 (2007).

[36] T. Mori, *Annual Review of Condensed Matter Physics* **14**, 35 (2023).

[37] A. Iserles, *Not. Am. Math. Soc.* **49** (2002).

[38] K. Khodjasteh and D. A. Lidar, *Phys. Rev. A* **78**, 012355 (2008).

[39] A. Parra-Rodriguez, P. Lougovski, L. Lamata, E. Solano, and M. Sanz, *Phys. Rev. A* **101**, 022305 (2020).

[40] T. Mostafaie, F. M. Khiyabani, and N. J. Navimipour, *Computers & Operations Research* **120**, 104850 (2020).

[41] P. Zanardi, *Physics Letters A* **258**, 77 (1999).

[42] A. R. Calderbank, E. M. Rains, P. W. Shor, and N. J. A. Sloane, *Quantum error correction via codes over $gf(4)$* (1997), [arXiv:quant-ph/9608006](https://arxiv.org/abs/quant-ph/9608006) [quant-ph].

[43] M. Stollsteimer and G. Mahler, *Phys. Rev. A* **64**, 052301 (2001).

[44] A. S. Hedayat, N. J. A. Sloane, and J. Stufken, *Orthogonal arrays: theory and applications* (Springer Science & Business Media, 2012).

[45] Orthogonal Arrays — neilsloane.com, <http://neilsloane.com/oadir/index.html>.

[46] P. Delsarte, *Information and Control* **23**, 407 (1973).

[47] M. F. Ezerman, S. Ling, and P. Sole, *IEEE Transactions on Information Theory* **57**, 5536 (2011).

[48] R. C. Bose and D. K. Ray-Chaudhuri, *Information and control* **3**, 68 (1960).

[49] D. Gorenstein and N. Zierler, *Journal of the Society for Industrial and Applied Mathematics* **9**, 207 (1961).

[50] B. Zeng, A. Cross, and I. L. Chuang, *IEEE Transactions on Information Theory* **57**, 6272 (2011).

[51] J. Haah, arXiv preprint arXiv:1607.01387 (2016).

[52] G. Burkard, T. D. Ladd, A. Pan, J. M. Nichol, and J. R. Petta, *Reviews of Modern Physics* **95**, 025003 (2023).

[53] X. Xue, M. Russ, N. Samkharadze, B. Undseth, A. Sammak, G. Scappucci, and L. M. K. Vandersypen, *Nature* **601**, 343 (2022).

[54] A. Noiri, K. Takeda, T. Nakajima, T. Kobayashi, A. Sammak, G. Scappucci, and S. Tarucha, *Nature* **601**, 338 (2022).

[55] A. R. Mills, C. R. Quinn, M. J. Gullans, A. J. Sigillito, M. M. Feldman, E. Nielsen, and J. R. Petta, *Science Advances* **8**, eabn5130 (2022).

[56] M. T. Nguyen, M. Rimbach-Russ, L. M. Vandersypen, and S. Bosco, arXiv preprint arXiv:2503.12182 [10.1103/kp8s-py9m](https://arxiv.org/abs/2503.12182) (2025).

[57] S. Geyer, B. Hetényi, S. Bosco, L. C. Camenzind, R. S. Egeli, A. Fuhrer, D. Loss, R. J. Warburton, D. M. Zumbühl, and A. V. Kuhlmann, *Nature Physics* **20**, 1152 (2024).

[58] J. Saez-Mollejo, D. Jirovec, Y. Schell, J. Kukucka, S. Calcaterra, D. Chrastina, G. Isella, M. Rimbach-Russ, S. Bosco, and G. Katsaros, *Exchange anisotropies in microwave-driven singlet-triplet qubits* (2024), [arXiv:2408.03224](https://arxiv.org/abs/2408.03224) [cond-mat.mes-hall].

[59] P. C. Fariña, D. Jirovec, X. Zhang, E. Morozova, S. D. Oosterhout, S. Reale, T.-K. Hsiao, G. Scappucci, M. Veldhorst, and L. M. K. Vandersypen, *Site-resolved magnon and triplon dynamics on a programmable quantum dot spin ladder* (2025), [arXiv:2506.08663](https://arxiv.org/abs/2506.08663).

[60] T.-K. Hsiao, P. Cova Fariña, S. D. Oosterhout, D. Jirovec, X. Zhang, C. J. van Diepen, W. I. L. Lawrie, C.-A. Wang, A. Sammak, G. Scappucci, M. Veldhorst, E. Demler, and L. M. K. Vandersypen, *Phys. Rev. X* **14**, 011048 (2024).

[61] S. P. Pedersen, K. S. Christensen, and N. T. Zinner, *Phys. Rev. Res.* **1**, 033123 (2019).

[62] T. Menke, W. P. Banner, T. R. Bergamaschi, A. Di Paolo, A. Vepsäläinen, S. J. Weber, R. Winik, A. Melville, B. M. Niedzielski, D. Rosenberg, K. Serniak, M. E. Schwartz, J. L. Yoder, A. Aspuru-Guzik, S. Gustavsson, J. A. Grover, C. F. Hirjibehedin, A. J. Kerman, and W. D. Oliver, *Phys. Rev. Lett.* **129**, 220501 (2022).

[63] C. Berke, E. Varvelis, S. Trebst, A. Altland, and D. P. DiVincenzo, *Nature communications* **13**, 2495 (2022).

[64] P. Nation, H. Paik, A. W. Cross, and Z. Nazario, The IBM quantum heavy hex lattice, <https://www.ibm.com/quantum/blog/heavy-hex-lattice> (2021).

[65] Google Quantum AI et al., *Nature* **638**, 920 (2025).

[66] E. Abbe, A. Shpilka, and M. Ye, *IEEE Transactions on Information Theory* **67**, 3251 (2020).

[67] S. Bosco and M. Rimbach-Russ, *Exchange-only spin-orbit qubits in silicon and germanium* (2024), [arXiv:2410.05461](https://arxiv.org/abs/2410.05461) [cond-mat.mes-hall].

[68] D. Sen and R. Chitra, *Phys. Rev. B* **51**, 1922 (1995).

[69] M. J. Gullans and J. R. Petta, *Phys. Rev. B* **100**, 085419 (2019).

[70] J. Qi, Z.-H. Liu, and H. Xu, *Scalable multi-qubit intrinsic gates in quantum dot arrays* (2024), [arXiv:2403.06894](https://arxiv.org/abs/2403.06894) [quant-ph].

[71] V. John, C. X. Yu, B. van Straaten, E. A. Rodríguez-Mena, M. Rodríguez, S. Oosterhout, L. E. Stehouwer, G. Scappucci, S. Bosco, M. Rimbach-Russ, et al., arXiv preprint arXiv:2412.16044 (2024).

[72] Q. Fu, R. Li, L. Guo, and G. Xu, *Finite Fields and Their Applications* **35**, 231 (2015).

[73] A. Blokhuis and A. Brouwer, *European Journal of Combinatorics* **25**, 161 (2004).

[74] D. Leung, *Journal of Modern Optics* **49**, 1199 (2002).

[75] J. H. Conway and N. J. A. Sloane, *Sphere packings, lattices and groups* (2013) vol. 290, Springer Science & Business Media.

[76] A. Kitaev, *Annals of Physics* **321**, 2 (2006), january Special Issue.

[77] Y.-H. Wu, L. C. Camenzind, P. Büttler, I. K. Jin, A. Noiri, K. Takeda, T. Nakajima, T. Kobayashi, G. Scappucci, H.-S. Goan, and S. Tarucha, *Simultaneous high-fidelity single-qubit gates in a spin qubit array* (2025), [arXiv:2507.11918](https://arxiv.org/abs/2507.11918) [quant-ph].

[78] C. Read, E. Serrano-Ensástiga, and J. Martin, *Quantum* **9**, 1661 (2025).

[79] C. Read, E. Serrano-Ensástiga, and J. Martin, *Dynamical decoupling of interacting spins through group factorization* (2025), [arXiv:2506.15382](https://arxiv.org/abs/2506.15382) [quant-ph].

[80] G. Quiroz and D. A. Lidar, *Phys. Rev. A* **88**, 052306 (2013).

[81] G. T. Genov, D. Schraft, N. V. Vitanov, and T. Halfmann, *Phys. Rev. Lett.* **118**, 133202 (2017).